た。その後，カウントした各ウロコのドット数をエクセルファイルへ出力し，個々のウロコ面積（mm^2）に換算した。

2－5）ウロコのTRAPおよびALP活性

　基質液添加後20℃で30分間反応させた後，測定した405nmの吸光度からブランク値を差し引いた吸光度を求めた。この吸光度をp-ニトロフェノール希釈系列より求めた校正曲線を用い30分間に脱リン酸化酵素により生じたp-ニトロフェノール量（nmol pNP produced）を求めた。その後，重量補正法では，反応時間（h）とウロコ1枚の重さ（mg）で生じたp-ニトロフェノール量を除して，単位時間（h）・単位重量（mg）当たりの酵素活性（nmol pNP produced/（mg scale×h））とした。一方，面積補正法では，反応時間（h）とウロコ1枚の面積（mm^2 scale）で生じたp-ニトロフェノール量を除して，単位時間（h）・単位面積（mm^2）当たりの酵素活性（nmol pNP produced/（mm^2 scale×h））とした。

2－6）ウロコの重量と面積の関連

　キンギョの各ウロコの重量と面積の関係を144枚（2個体）について調べた。

2－7）ウロコの重量または面積とALPおよびTRAP活性の関連

　キンギョの片側のウロコのALP（24枚）およびTRAP（24枚）活性（nmol pNP produced/h）とそれぞれのウロコ重量（mg）を測定し，同じ個体の対側の対称位置のウロコのALP（24枚）およびTRAP（24枚）活性（nmol pNP produced/h）とそれぞれのウロコ面積（mm^2）を4個体について測定した。そして，ウロコの重量とALPまたはTRAP活性との関連とウロコの面積とALPまたはTRAP活性との関連を調べた。

2－8）重量補正法と面積補正法との関連

　ALPおよびTRAP活性のそれぞれについて，単位重量当たりの活性値（従来法）と単位面積当たりの活性値（改良法）との間の相関関係を調べた。

2－9）ウロコの面積と単位面積当たりのALPおよびTRAP活性との関連

　ウロコの面積でALPまたはTRAP活性値（nmol pNP produced/h）を除して算出した単位面積当たりのALPまたはTRAP活性値（nmol pNP produced/（mm^2 scale×h））とウロコの面積（mm^2）との関連から，単位面積当たりの活性に変換した効果を調べた。

3）統計処理

　結果はすべて平均値±標準誤差（standard error of mean: SEM）の形で表した。ウロコの重量と面積の関連は，ウロコの面積を目的変数，ウロコの重量を説明変数とする回帰分析を行った。ウロコの重量または面積とALPおよびTRAP活性の関連は，ウロコの酵素活性を目的変数，ウロコの重量あるいは面積を説明変数とする回帰分析を行った。重量補正法と面積補正法との関連は，単位面積当たりの活性値（改良法）を目的変数，単位重量当たりの活性値（従来法）を説明変数とする回帰分析を行った。ウロコの面積と単位面積当たりのALPおよびTRAP活性との関連は，単位面積当たりのALPおよびTRAP活性を目的変数，ウロコの面積を説明変数とする回帰分析を行った。危険率5％未満を統計学的有意水準とした。

Ⅲ．結　果

1）ウロコの重量と面積の関連

　各ウロコの重量と面積の間には，正の相関が見られた（$r = 0.65$，$p < 0.001$），（図5）。
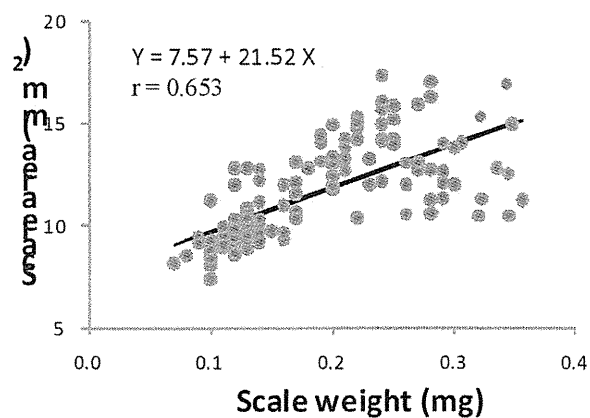

Y = 7.57 + 21.52 X
r = 0.653

図5　ウロコの重量と面積の関連．
Fig. 5　Correlation analysis between scale weight and scale area.

2）ウロコのTRAPまたはALP活性と重量または面積との関連

　ウロコ1枚のALP総活性とウロコの重さの間には，正の相関が見られた（$r = 0.57$，$p < 0.001$），（図6A）。また，TRAP総活性とウロコの重さの間にも，正の相関（$r = 0.65$，$p < 0.001$）が見られた（図6 B）。

ウロコ1枚のALP総活性とウロコの面積の間には，強い正の相関が見られた（$r = 0.91$, $p < 0.001$）（図6C）。また，TRAP総活性とウロコの面積の間にも，強い正の相関（$r = 0.78$, $p = 2.6 \times 10^{-22}$）が見られた（図6D）。

3）重量補正法と面積補正法との関連

単位重量当たりのALP活性値（従来法）と単位面積当たりのALP活性値（改良法）との間には，弱い正の相関（$r = 0.38$, $p < 0.001$）（図7A）が見られた。また，単位重量当たりのTRAP活性値（従来法）と

単位面積当たりのTRAP活性値（改良法）との間にも，正の相関（$r = 0.67$, $p < 0.001$）（図7B）が見られた。

4）ウロコの面積と単位面積当たりのALPおよびTRAP活性との関連

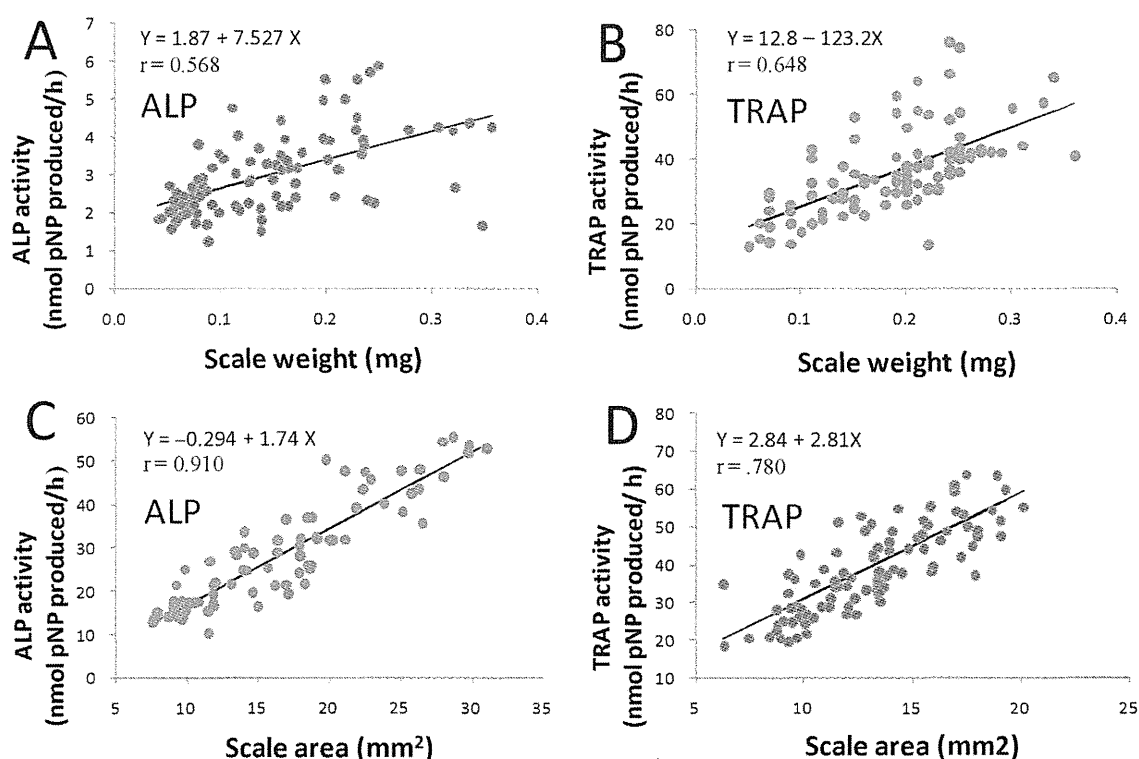ウロコのALPおよびTRAP活性を単位面積当たりの活性で表すと，ウロコの面積に関係なくほぼ一定となった（図8A, B）。

図6　ウロコのTRAPまたはALP活性とその重量または面積との関連.

Fig. 6　Correlation analyses (A: scale weight vs ALP activity; B scale weight vs TRAP activity; C: scale area vs ALP activity; D: scale area vs TRAP activity).
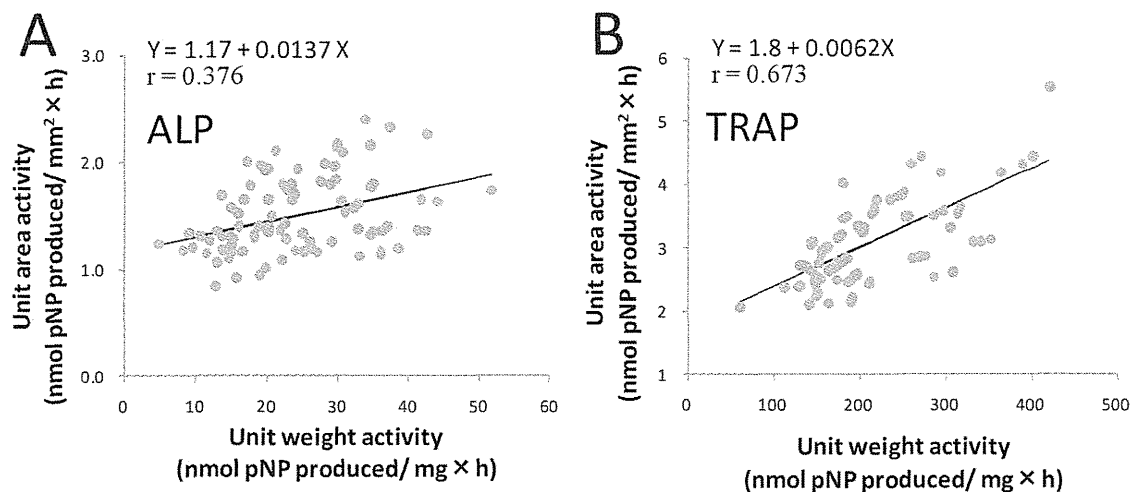
A

$Y = 1.17 + 0.0137\,X$
$r = 0.376$

ALP

Unit area activity
(nmol pNP produced/ mm² × h)

Unit weight activity
(nmol pNP produced/ mg × h)

B

$Y = 1.8 + 0.0062X$
$r = 0.673$

TRAP

Unit area activity
(nmol pNP produced/ mm² × h)

Unit weight activity
(nmol pNP produced/ mg × h)

図7　重量補正法と面積補正法との関連．（A）単位重量当たりのALP活性値（従来法）と単位面積当たりのALP活性値（改良法）との相関．（B）単位重量当たりのTRAP活性値（従来法）と単位面積当たりのTRAP活性値（改良法）との相関．

Fig. 7　Correlation analysis between weight-correction method and areal-correction method. Left panel (A) showed correlation between unit weight ALP activity (conventional method) and unit area ALP activity (improved method). Right panel (B) showed correlation between unit weight TRAP activity (conventional method) and unit area TRAP activity (improved method).
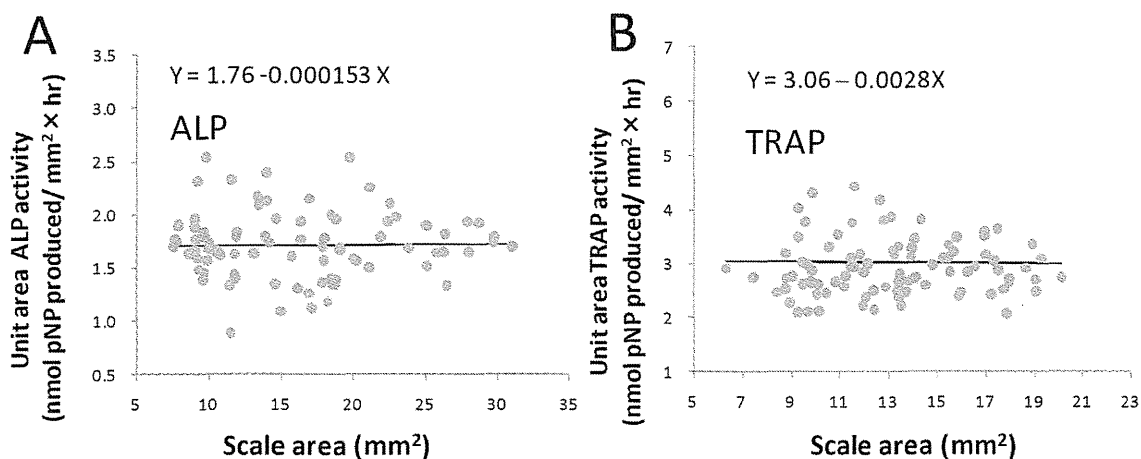

A

$Y = 1.76 - 0.000153\,X$

ALP

Unit area ALP activity
(nmol pNP produced/ mm² × hr)

Scale area (mm²)

B

$Y = 3.06 - 0.0028X$

TRAP

Unit area TRAP activity
(nmol pNP produced/ mm² × hr)

Scale area (mm²)

図8　ウロコの面積と単位面積当たりのALPおよびTRAP活性との関連．（A）ウロコの面積と単位面積当たりのALP活性との関連．（B）ウロコの面積と単位面積当たりのTRAP活性との関連．

Fig. 8　Relationship between scale area and enzyme activities. Left panel (A) showed relationship between scale area and unit area ALP activity. Right panel (B) showed relationship between scale area and unit area TRAP activity.

Ⅳ．考　察

　従来ウロコのALPおよびTRAP活性をウロコの重量（mg）当たりの活性で表していた方法では，ウロコの乾燥と1枚1枚の秤量に多大な時間を要したことと，1mg未満の乾燥ウロコの秤量に困難さがあった

ため，ウロコのALPおよびTRAP活性をウロコの面積（mm²）当たりの活性で表す方法を今回検討した。これまで96穴プレート1枚当たり約2時間程度かかっていた乾燥ウロコ重量測定時間が，ウロコの乾燥を待つことなく約5分程度の面積測定時間に短縮された。また，ウロコ面積は，画像処理ソフトによる自

動測定なので，誰が何度やっても同じ値となり，正確度と再現性が著しく向上した。さらに，これまで困難であった小さなウロコの測定も1枚ごとに容易に測定できるようになった。

ウロコの重量と面積の間には，正の相関があるものの，ウロコ重量が0.22 mg以上では，ウロコの重量と面積との相関が低下する傾向が見られた。また，ウロコの重量とALPおよびTRAP総活性値の間には，共に正の相関があるものの，ウロコの面積とALPおよびTRAP総活性値の間には，より強い正の相関があった。これは，ウロコの重量は，石灰化層や繊維層の厚さにより大きく影響され，必ずしもウロコサイズと一致しないことと，ウロコの破骨細胞や骨芽細胞が，ウロコの中に3次元的に分布しているのではなく，ウロコ表面に2次元的に分布している（Azuma, et al. 2007）ことが影響したものと思われた。したがって，ウロコのALPおよびTRAP活性のウロコサイズによる影響をなくすには，単位面積あたりの酵素活性表示が適するものと思われた。

ALPおよびTRAP活性の重量補正法（従来法）と面積補正法（改良法）との間には，相関関係が見られた（図7）。したがって，今後ウロコのALPおよびTRAP活性を単位面積当たりによる面積補正法で表しても従来法で測定した値との間に互換性が期待できる。また，ALPおよびTRAP活性を面積補正法で算出した単位面積当たりの活性で表すと，ALPおよびTRAP活性は，ウロコの表面積と無相関でウロコサイズによる影響が無くなったことが明らかになった（図8）。

キンギョのウロコは，抜去しても再生する。そうしてできた再生ウロコは，普通のウロコにくらべてALP活性が統計学的に有意に高く，さらにエストロゲン（E2）のような骨代謝に関連するホルモン刺激に対しても，普通ウロコよりも感度良く，有意に高いALP活性の上昇を示すことが報告されている（Yoshikubo, et al. 2005）。このように骨代謝に影響する刺激に対して優れた感度を示す再生ウロコを骨のモデルとして用いる方が，普通ウロコを用いるよりも高感度のウロコアッセイができると考えられる。その際，石灰化層や繊維層が薄く軽い再生ウロコのウロコ1枚当たりの酵素活性を求める方法としては，重量法よりも面積法が適するものと思われる。そして，再生ウロコの系を用い，今回検討した面積補正法を利用した酵素活性測定法を利用することにより，今後の海域汚染物質による骨代謝への影響を感度良く評価することに寄与できるものと思われる。

V. まとめ

われわれは，ウロコを骨モデルとした破骨細胞および骨芽細胞活性測定法を，従来から行ってきたウロコの重量当たりの酵素活性測定法から，ウロコの面積当たりの酵素活性測定法への変更を検討した。その結果，面積の自動計測によるウロコの面積当たりの酵素活性測定法への変更により，①酵素活性測定時間の大幅な短縮，②酵素活性測定の正確度および再現性の向上，③ウロコ1枚からの酵素活性測定，④酵素活性測定へのウロコサイズの影響を軽減が実現でき，⑤重量補償補正法との相関関係も確認した。

文　献

Azuma, K., Kobayashi, M., Nakamura, M., Suzuki, N., Yashima, S., Iwamuro, S., Ikegame, M., Yamamoto, T. and Hattori, A., 2007: Two osteoclastic markers expressed in multinucleate osteoclasts of goldfish scales. *Biochem. Biophys. Res. Commun.*, **362**, 594-600.

Bereiter-Hahn, J. and Zylberberg, L., 1993: Regeneration of teleost fish scale. *Comp. Biochem. Physiol.*, **105A**, 625-641.

Dimai, H. P., Linkhart, T. A., Linkhart S. G., Donahue, L. R., Beamer, W. G., Rosen, C. J., Farley, J. R. and Baylink, D. J., 1998: Alkaline phosphatase levels and osteoprogenitor cell numbers suggest bone formation may contribute to peak bone density differences between two inbred strains of mice. *Bone*, **22**, 211-216.

Kitamura, K., Suzuki, N., Sato, Y., Nemoto, T., Ikegame, M., Yamamoto, T., Shimizu, N., Kondo, T., Furusawa, Y., Shigehito Wada, S. and Hattori, A., 2010a: Osteoblast activity in the goldfish scale responds sensitively to mechanical stress. *Comp. Biochem. Physiol. A*, **156**,

357-363.

Kitamura, K., 2010b: Effects of low-intensity ultrasound on osteoblasts and osteoclasts in goldfish scale. *Biological Sciences in Space*, **24**, 29-34.

Lehane, D. B., Mckie, N., Russell, R. G. and Henderson, I. W., 1999: Cloning of a fragment of the osteonectin gene from goldfish, *Carassius auratus*: its expression and potential regulation by estrogen. *Gen. Comp. Endocrinol.*, **114**, 80-87.

Nishimoto, S. K., Araki, N., Robinson, F. D. and Waite, J. H., 1992: Discovery of bone γ-carboxyglutamic acid protein in mineralized scales. *J. Biol. Chem.*, **267**, 11600-11605.

Suzuki, N., Suzuki, T. and Kurokawa, T., 2000: Suppression of osteoclastic activities by calcitonin in the scales of goldfish (freshwater teleost) and nibbler fish (seawater teleost). *Peptides*, **21**, 115-124.

Suzuki, N. and Hattori, A., 2002: Melatonin suppresses osteoclastic and osteoblastic activities in the scales of goldfish. *J. Pineal Res.*, **33**, 253-258.

Suzuki, N., Kitamura, K., Somei, M., Reiter, R. J. and Hattori, A., 2008: Novel bromomelatonin derivatives suppress osteoclastic activity and increase osteoblastic activity: Implications for the treatment of bone diseases. *J. Pineal Res.*, **44**, 326-334.

Vaes, G., 1988: Cellular biology and biochemical mechanism of bone resorption. A review of recent developments on the formation, activation, and mode of action of osteoclasts. *Clin. Orthop. Relat. Res.*, **231**, 239-271.

Yoshikubo, H., Suzuki, N., Takemura, K., Hoso, M., Yashima, S., Iwamuro, S., Takagi, Y., Tabata, M.J. and Hattori, A., 2005: Osteoblastic activity and estrogenic response in the regenerating scale of goldfish, a good model of osteogenesis. *Life Sci.*, **76**, 2699-2709.

Effects of Inorganic Mercury on Osteoclasts and Osteoblasts of the Goldfish Scales *In Vitro*

Nobuo SUZUKI[1]*, Koji YACHIGUCHI[2], Kazuichi HAYAKAWA[3], Katsunori OMORI[4], Koji TAKADA[5],
Makoto J. TABATA[6], Kei-Ichiro KITAMURA[7], Masato ENDO[8], Shigehito WADA[9],
Ajai K. SRIVASTAV[10], Vishwajit S. CHOWDHURY[11], Yuji OSHIMA[12]
and Atsuhiko HATTORI[13]

Department of Bioscience and Biotechnology, Graduate School of Bioresource and
Bioenvironmental Sciences, Kyushu University, Hakozaki 6–10–1,
Higashi–ku, Fukuoka, 812–8581, Japan
(*Received October 26, 2010 and accepted November 8, 2010*)

The fish scales are the major source of internal calcium requirement due to having a higher internal calcium reservoir than the body skeleton during the periods of drastic calcium demand, such as sexual maturation. Therefore, we developed original *in vitro* assay system using goldfish scales that contain osteoclasts and osteoblasts, and examined the direct effect of inorganic mercury ($HgCl_2$) on osteoclasts and osteoblasts. In this assay system, we measured the activities of tartrate–resistant acid phosphatase (TRAP) and alkaline phosphatase (ALP) as respective indicators of each activity in osteoclasts and osteoblasts. TRAP activity in the scales significantly decreased by the treatment of $HgCl_2$ (10^{-5} to 10^{-4} M) during 6 hrs of incubation. In addition, mRNA expressions of osteoclastic markers: TRAP and cathepsin K significantly decreased compared with control. In our knowledge, this is the first report of a direct effect of inorganic mercury on osteoclasts. On the other hand, ALP activity decreased after exposures of $HgCl_2$ at a concentration of 10^{-6}, 10^{-5} or 10^{-4}M for 36 and 64 hrs, although its activity did not change after 6 and 18 hrs. The mRNA expression of metallothionein (MT) which is a metal–binding–protein that protects the organism from heavy metal, significantly increased by $HgCl_2$ (10^{-4}M) although insulin–like growth factor–I (osteoblastic marker) was less than those of control scales by treatment with $HgCl_2$ (10^{-4}M). These results suggests that osteoblasts may synthesize MT and protect from mercury until 18 hrs incubation. Thus, the scale *in vitro* assay system would be a useful means for analysis of heavy metal on bone metabolism.

Keywords: inorganic mercury, *in vitro* assay, osteoclasts, osteoblasts, scales

INTRODUCTION

Heavy metals such as mercury, cadmium and copper are known to be extremely toxic to organisms. Mercury has been recognized as an environmental contaminant since the Minamata disaster in the late 1950s. Minamata disease which was caused by the consumption of marine fishes severely polluted with mercury from local industrial discharge due to this Minamata disaster (Takeuchi *et al.*, 1978; Takeuchi, 1982). This extremely adverse situation occurred because of mercury, a highly toxic compound, was severely bio–accumulated (in case of long–

finned eels: approx. 1,000,000 times higher than environmental water) by fish (Redmayne *et al.*, 2000).

The effect of mercury on the central nervous system has widely studied and revealed that mercury is a neuro–toxic material, and its poisoning effect is characterized by the damage in discrete portions of the brain, such as the visual cortex and the granule layer of the cerebellum (Castoldi *et al.*, 2001). As bio–accumulation of mercury in bone is lower than that in neural tissues (Boyer *et al.*, 1978; Doyle, 1979; Berglund *et al.*, 2000), much attention has not been given to bone in this area of research.

Recently, Lake *et al.* (2006) reported that the corre-

[1] Noto Marine Laboratory, Institute of Nature and Environmental Technology, Kanazawa University, Housu–gun, Ishikawa 927–0553, Japan
[2] Noto Marine Center, Housu–gun, Ishikawa 927–0552, Japan
[3] Graduate School of Natural Science and Technology, Kanazawa University, Kakuma, Ishikawa 920–1192, Japan
[4] Japan Aerospace Exploration Agency, Tsukuba, Ibaraki 305–8505, Japan
[5] Department of Biochemistry, Jikei University School of Medicine, Minato–ku, Tokyo 105–8461, Japan
[6] Section of Biostructural Science, Graduate School of Tokyo Medical and Dental University, Bunkyo–ku, Tokyo 113–8549, Japan
[7] Faculty of Health Sciences, Institute of Medical, Pharmaceutical and Health Sciences, Kanazawa University, Kanazawa, Ishikawa 920–0942, Japan
[8] Department of Marine Biosciences, Faculty of Marine Science, Tokyo University of Marine Science and Technology, Konan, Minato–ku, Tokyo 108–8477, Japan
[9] Department of Oral and Maxillofacial Surgery, Faculty of Medicine, University of Toyama, Sugitani, Toyama 930–0194, Japan
[10] Department of Zoology, University of Gorakhpur, Gorakhpur 273009, India
[11] International Education Center, Department of Bioresource Sciences, Faculty of Agriculture, Kyushu University, Fukuoka 812–8581, Japan
[12] Department of Bioscience and Biotechnology, Graduate School of Bioresource and Bioenvironmental Sciences, Kyushu University, Hakozaki 6–10–1, Higashi–ku, Fukuoka, 812–8581, Japan
[13] Department of Biology, College of Liberal Arts and Sciences, Tokyo Medical and Dental University, Ichikawa, Chiba 272–0827, Japan
* Corresponding author (E–mail: nobuo@kenroku.kanazawa–u.ac.jp)

lation between the total mercury concentration of the scales and that of the muscles was high (r=0.89), and suggested the suitability for prediction of muscle tissue by the assessment of available mercury in the fish scales. It is known that the scales are calcified tissue which contains osteoclasts and osteoblasts (Bereiter–Hahn and Zylberberg, 1993; Suzuki et al., 2000; Yoshikubo et al., 2005; Suzuki et al., 2007) and is reported that the scales are a better potential internal calcium reservoir than the body skeletons, jaws and otolithes, examined by the ^{45}Ca–labelling study for the calcified tissues of goldfish and killifish (Mugiya and Watabe, 1977). In fishes, thus, the scale accumulates mercury and seems to be a sensitive tissue for mercury.

Recently, we have developed a novel in vitro assay system using goldfish scale (Suzuki et al., 2000; Suzuki and Hattori, 2002) because the scale is a very active tissue of calcium regulation in fish described above. In the present study, therefore, we examined the effect of inorganic mercury (HgCl$_2$) on the scale osteoclasts and osteoblasts. To confirm the effects of HgCl$_2$ on osteoclasts and osteoblasts, the mRNA expressions of osteoclastic markers (tartrate–resistant acid phosphatase: TRAP and cathepsin K) and osteoblastic marker (insulin–like growth factor–I: IGF–I) were investigated using reverse–transcription (RT)–PCR. Furthermore, the mRNA expression of metallothionein (MT), which is a metal–binding–protein that protects the organism from heavy metal (Hamer, 1986; Klaassen et al., 1999), was also examined using RT–PCR.

MATERIALS AND METHODS

Animals

Our previous study (Suzuki et al., 2000) indicated that the sensitivity for calcemic hormone such as estrogen and calcitonin was higher in mature female than mature male in goldfish (Carassius auratus). Therefore, mature female goldfish (n=12, 35.50 ± 1.30 g) were purchased from commercial source (Higashikawa Fish Farm, Yamatokoriyama, Japan) and used in the scale in vitro assay. All experimental procedures were conducted in accordance with the Guide for the Care and Use of Laboratory Animals of Kanazawa University.

Effect of HgCl$_2$ on TRAP and ALP activities in the cultured scales of goldfish

A 1% penicillin–streptomycin mixture (ICN Biomedicals Inc., OH, USA) was added to Eagle's minimum essential medium (MEM; ICN Biomedicals Inc.). HEPES (Research Organics Inc., OH, USA) (20 mM) was added into MEM and adjusted to pH 7.0. After filtration, MEM was used in this experiment for analyzing the effect of HgCl$_2$ on TRAP and ALP activities in the cultured goldfish scales. Scales collected from goldfish under anesthesia with ethyl 3–aminobenzoate, methanesulfonic acid salt (MS–222, Sigma–Aldrich, Inc., MO, USA) and incubated for 6 hrs in MEM supplemented with 10^{-8}–10^{-4} M HgCl$_2$ (Wako Pure Chemical Industries, Ltd., Osaka, Japan) and compared with control (HgCl$_2$–free medium).

To evaluate the effect of HgCl$_2$ on osteoclasts and osteoblasts, furthermore, scales were incubated with HgCl$_2$ (10^{-7}, 10^{-6}, 10^{-5}, and 10^{-4} M) for comparatively longer exposure times, namely 18, 36, and 64 hrs. After incubation, scales were fixed in 10% formalin in a 0.05 M cacodylate buffer (pH 7.4) followed by a storage in a 0.05 M cacodylate buffer at 4 °C until analysis.

The measurement methods of TRAP and ALP activities have been described by Suzuki and Hattori (2002). We detected the respective enzyme activity from one scale by transferring each scale into a 96–well–microplate and directly incubating it with the substrate in each well. The procedure of TRAP measurement was as follows. Each scale was transferred to its own well in a 96–well microplate after measurement of the scale weight. An aliquot of 200 μl of 10 mM para–nitrophenyl-phosphate and 20 mM tartrate in a 0.1 M sodium acetate buffer (pH 5.3) was added to each well. This plate was then incubated at 20 °C for 30 min while being shaken. After incubation, the reaction was stopped by adding 50 μl of 2 N NaOH. One hundred and fifty μl of a colored solution was transferred to a new plate, and the absorbance was measured at 405 nm. The absorbance was converted into the amount of produced para–nitrophenol (pNP) using a standard curve for pNP. The results are shown as means ± SEM of eight scales.

ALP activities were measured using an alkaline buffer (100 mM Tris–HCl, pH 9.5; 1 mM MgCl$_2$; 0.1 mM ZnCl$_2$). Other conditions were the same as those for the measurement of TRAP activity.

Changes of TRAP, cathepsin K, IGF–I, and MT mRNA expression in HgCl$_2$–treated scales for 18 hrs of culture

Scales were collected from goldfish under anesthesia with MS–222. To examine changes in TRAP, cathepsin K, IGF–I, and MT mRNAs that responded to HgCl$_2$, these scales were incubated for 18 hrs in MEM (containing antibiotic and 20 mM HEPES) supplemented with HgCl$_2$ (10^{-4} M) and compared with the control (without metals). We previously reported that IGF–I mRNA expression decreased at 18 hrs of incubation (Suzuki and Hattori, 2003). Therefore, this incubation period was adopted. After incubation, the scales were frozen at −80 °C for mRNA analysis.

Total RNAs were prepared from the goldfish scales using a total RNA isolation kit (Nippon Gene, Tokyo, Japan). RT–PCR was performed using Oligotex–dT 30 Super (Takara Bio Inc., Otsu, Japan) as an oligo dT primer to prevent genomic DNA contamination (Suzuki et al., 1997). The gene–specific primers (TRAP 5': AACTTC-CGCATTCCTCGAACAG; TRAP 3': GGCCAGCCACCAGGAGATAA; cathepsin K 5': GCTAT-GGAGCCACACCAAAAGG; cathepsin K 3': CTGCGCTTCCAGCTCTCACAT) reported by Azuma et al. (2007) were used. IGF–I and MT cDNAs were also amplified using gene specific primers (IGF–I 5': GGAGACGCTGTGCGGG; IGF–I 3': CCTCAGCTCACAGCTCTG; MT 5': ATGGATCCGTGCGAATGC; MT 3':

CTCCTCATTGACAGCAGCT). These were designed from the nucleotide sequences of respective cDNA (IGF–I: Kermouni *et al.*, 1998; MT: Chan, 1994). β–actin cDNA using a primer set (5':CACTGTGCCCATCTACGAG; 3': CCATCTCCTGCTCGAAGTC) (Chan *et al.*, 1998) were also amplified. The conditions for PCR amplification were denaturation for 0.5 min at 96 °C, annealing for 1 min at 55 °C, and extension for 2 min at 72 °C, followed by a single cycle at 72 °C for 30 min. The cycle numbers for the amplification in TRAP, cathepsin K, IGF–I, MT, and β–actin cDNAs were determined by ensuring that PCR amplification was at submaximum and the intensity of the band corresponded exactly to the amount of starting material. The PCR products were analyzed on a 2.5% NuSive GTG agarose gel (FMC BioProducts, ME, USA) and stained with ethidium bromide. The band densities were estimated using a computer program (NIH Image J). The mRNA levels of TRAP, cathepsin K, IGF–I and

MT were normalized to the mRNA level of β–actin.

Statistical analysis

The statistical significance was assessed by one–way ANOVA followed by Dunnett test. The significance level chosen was as $P<0.05$.

RESULTS

Effect of HgCl₂ on TRAP activity in the cultured scales of goldfish

HgCl₂ was significantly decreased the TRAP activities of the scales by 6 hrs of incubation ($P<0.01$ for 10^{-5} M; $P<0.001$ for 10^{-4} and 10^{-3}M) (Fig. 1). Thus, increased doses of HgCl₂ resulted in greater effects on decreasing TRAP activities dose–dependently.

By the long incubation time period (18 to 64 hrs), only at 10^{-4}M, significant difference ($P<0.01$) between HgCl₂–treated scales and control scales was obtained by
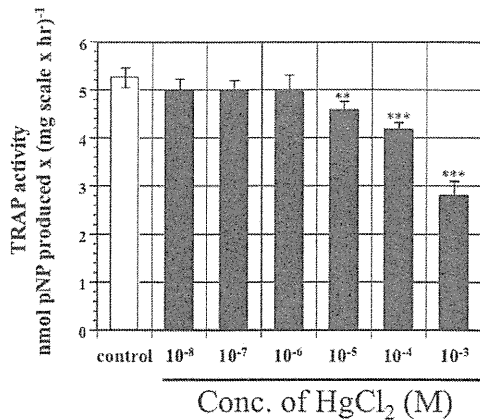

Fig. 1. Effect of HgCl₂ (10^{-8} to 10^{-3}M) on TRAP activity in the cultured scales incubated for 6 hrs. **, *** indicate statistically significant differences at $P<0.01$ and $P<0.001$, respectively, from the value in the control scales.
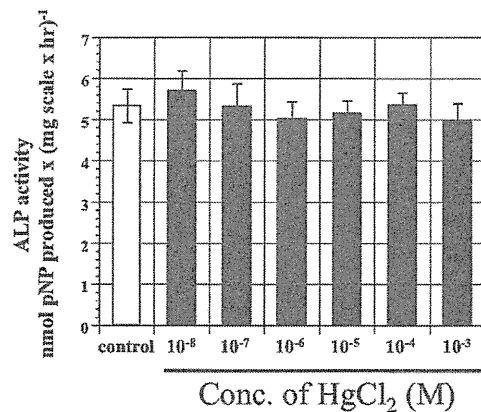

Fig. 3. Effect of HgCl₂ (10^{-8} to 10^{-3}M) on ALP activity in the cultured scales incubated for 6 hrs. There was no significant difference between HgCl₂–treated scales and control scales.
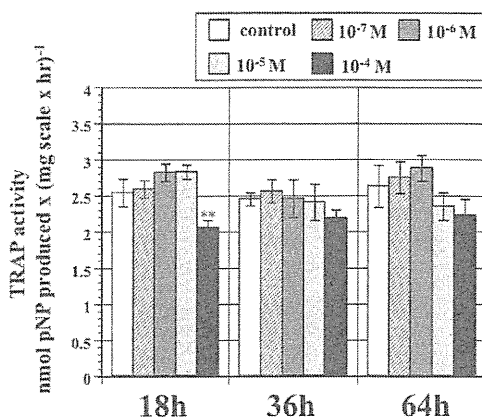

Fig. 2. Effect of HgCl₂ (10^{-7} to 10^{-4}M) on TRAP activity in the cultured scales incubated for 18, 36, and 64 hrs. ** indicates statistically significant difference at $P<0.01$ from the values in the control scales.
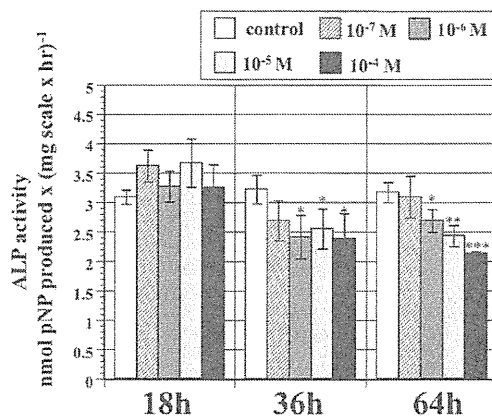

Fig. 4. Effect of HgCl₂ (10^{-7} to 10^{-4}M) on ALP activity in the cultured scales incubated for 18, 36, and 64 hrs. *, **, *** indicate statistically significant differences at $P<0.05$, $P<0.01$ and $P<0.001$, respectively, from the values in the control scales.

18 hrs of incubation (Fig. 2).

Effect of HgCl₂ on ALP activity in the cultured scales of goldfish

The ALP activity of the control scales by 6 hrs of incubation was 5.33 ± 0.41 (nmol produced pNP/mg scale/hr) which did not show any difference with HgCl₂-treated groups (10^{-8} to 10^{-4}M) (Fig. 3). Thus, the ALP activity did not change during 6 hrs of incubation with HgCl₂ compared to the control.

However, the ALP activity in the HgCl₂-treated scales decreased significantly by 36 hrs ($P<0.05$ for 10^{-6}M, 10^{-5}M or 10^{-4}M) and 64 hrs ($P<0.05$ for 10^{-6}M; $P<0.01$ for 10^{-5}M and $P<0.001$ for 10^{-4}M) of incubation from the values of the control scales although it did not change at 18 hrs of incubation (Fig. 4).

Changes of TRAP, cathepsin K, IGF–I, and MT mRNA expression in HgCl₂-treated scales

After 18 hrs of incubation, the mRNA expressions of TRAP, cathepsin K and IGF–I in HgCl₂-treated scales were significantly ($P<0.001$ for TRAP; $P<0.001$ for cathepsin K and $P<0.001$ for IGF–I) lower than those in the control scales (Fig. 5). Conversely, the mRNA expression was significantly ($P<0.001$) increased for MT when treated with HgCl₂ (Fig. 5).
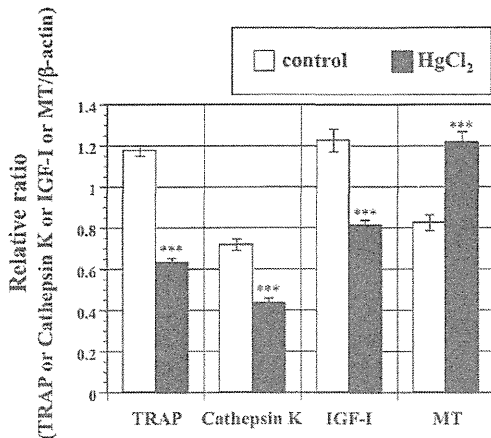

Fig. 5. Changes in the mRNA expression of TRAP, cathepsin K, IGF–I, and MT in HgCl₂ (10^{-4}M)–treated scales of goldfish incubated for 18 hrs of culture. *** indicates statistically significant difference at $P<0.001$ from the values in the control scales.

DISCUSSION

The present study demonstrated that fish scale sensitively responded to HgCl₂. A high co-relation of mercury between scales and muscles was reported in largemouth bass (Lake et al., 2006). This indicates that accumulation of mercury is occurred in the fish scale although mercury did not accumulate in the vertebral bone of fish (Camusso et al., 1995). It is also well-known that the scale is a more active tissue in fish calcium regulation than vertebral bone (Mugiya and Watabe, 1977; Yamada,

1961; Berg, 1968; Bereiter–Hahn and Zylberberg, 1993). Therefore, we strongly believe that the fish scale is capable to accumulate mercury and respond to mercury similarly like calcium.

In mammals, the influence of mercury on bone metabolism has been studied only by *in vivo* experiments and investigated in bone formation or osteoblastic activity (Yonaga et al., 1985; Jin et al., 2002). Mercury inhibited the growth of tibia in rats (Yonaga et al., 1985) and decreased serum levels of osteoblastic markers (ALP and osteocalcin) (Jin et al., 2002). In our knowledge, our study is the first to indicate direct effect of inorganic mercury on osteoclasts. The inhibitory action of HgCl₂ on osteoclasts after 6 hrs incubation was stronger than that of 18 to 64 hrs incubation. As for organic mercury, similar results were obtained in our scale assay system (Suzuki et al., 2004). Furthermore, we recently succeed to clone osteoclastic markers: TRAP and cathepsin K in fish for the first time (Azuma et al., 2007) and examined mRNA expressions of these markers in the HgCl₂-treated scales. In the present study, we confirmed that the both mRNA expressions of TRAP and cathepsin K decreased as TRAP enzyme activity did.

It was found that the mRNA expression of MT in HgCl₂-treated scales increased in the present study. This result is similar to that in mammals because it has been demonstrated that MT plays a protective role in mercury–induced toxicity in bone (Jin et al., 2002). Fish are aquatic animals with scales that are always exposed to environmental water. In an *in vitro* experiment for 6 and 18 hrs of incubation, therefore, osteoblasts may be resistant to mercury as a result of MT production. On the other hand, IGF–I mRNA expression decreased compared to the control. As IGF–I participates in osteoblastic growth and differentiation, we speculated that mercury has toxic effect on osteoblasts under long–term exposure.

We previously demonstrated that the osteogenesis of regenerating scale is very similar to that of mammalian membrane bone and a good model of osteogenesis (Yoshikubo et al., 2005). Using this system, furthermore, we first demonstrated that calcitonin, a hypocalcemic hormone, suppressed osteoclastic activity in teleosts as well as in mammals (Suzuki et al., 2000) and that melatonin, a major hormone secreted from the pineal gland, suppressed the functions in both osteoclasts and osteoblasts (Suzuki and Hattori, 2002). Osteoblasts in the scale responded to estrogen as they do in mammals (Yoshikubo et al., 2005). In addition, the effects of endocrine disrupters, such as bisphenol–A (Suzuki and Hattori, 2003) and tributyltin (Suzuki et al., 2006), and heavy metals, i.e., cadmium and organic mercury (Suzuki et al., 2004), on osteoblasts and osteoclasts have been examined. Moreover, we indicated that cadmium (even at 10^{-11}M) responded to TRAP activity in the scale (Suzuki et al., 2004). Considering these results together with present data, our scale assay system will be useful for analysis of environmental contaminant on bone metabolism.

REFERENCES

Azuma, K., M. Kobayashi, M. Nakamura, N. Suzuki, S. Yashima, S. Iwamuro, M. Ikegame, T. Yamamoto and A. Hattori 2007 Two osteoclastic markers expressed in multinucleate osteoclasts of goldfish scales. *Biochem. Biophys. Res. Commun.*, **362**: 594–600

Bereiter–Hahn, J. and L. Zylberberg 1993 Regeneration of teleost fish scale. *Comp. Biochem. Physiol.*, **105A**: 625–641

Berg, A. 1968 Studies on the metabolism of calcium and strontium in freshwater fish. I. Relative contribution of direct and intestinal absorption. *Mem. Ist. Ital. Idrobiol.*, **23**: 161–196

Berglund, M., A. Åkesson, P. Bjellerup and M. Vahter 2000 Metal–bone interactions. *Toxicol. Lett.*, **112–113**: 219–225

Boyer, C. I. Jr., E. J. Andrews, A. deLahunta, C. A. Bache, W. H. Gutenmann and D. J. Lisk 1978 Accumulation of mercury and selenium in tissues of kittens fed commercial cat food. *Cornell. Vet.*, **68**: 365–374

Camusso, M., L. Vigano and R. Balestrini 1995 Bioconcentration of trace metals in rainbow trout: A field study. *Ecotxicol. Environ. Saf.*, **31**: 133–141

Castoldi, A. F., T. Coccini, S. Ceccatelli and L. Manzo 2001 Neurotoxicity and molecular effects of methylmercury. *Brain Res. Bull.*, **55**: 197–203

Chan, K.–M. 1994 PCR–cloning of goldfish and tilapia metallothionein complementary DNAs. *Biochem. Biophys. Res. Commun.*, **205**: 368–374

Chan, K.–W., K.–L. Yu, J. Rivier and B. K.–C, Chow 1998 Identification and characterization of a receptor from goldfish specific for a teleost growth hormone–releasing hormone–like peptide. *Neuroendocrinology*, **68**: 44–56

Doyle, J. J. 1979 Toxic and essential elements in bone: A review. *J. Anim. Sci.*, **49**: 482–497

Hamer, D. H. 1986 Metallothionein. *Annu. Rev. Biochem.*, **55**: 913–951

Jin, G.–B., S. Inoue, T. Urano, S. Cho, Y. Ouchi and J.–C. Cyong 2002 Induction of anti–metallothionein antibody and mercury treatment decreases bone mineral density in mice. *Toxcol. Appl. Pharmacol.*, **185**: 98–110

Kermouni, A., S. S. Mahmoud, S. Wang, M. Moloney and H. R. Habibi 1998 Cloning of a full–length insulin–like growth factor–I complementary DNA in the goldfish liver and ovary and development of a quantitative PCR method for its measurement. *Gen. Comp. Endocrinol.*, **111**: 51–60

Klaassen, C. D., J. Liu and S. Choudhuri 1999 Metallothionein: An intracellular protein to protect against cadmium toxicity. *Annu. Rev. Pharmacol. Toxicol.*, **39**: 267–294

Lake, J. L., S. A. Ryba, J. R. Serbst and A. D. Libby 2006 Mercury in fish scales as an assessment method for predicting muscle tissue mercury concentrations in largemouth bass. *Arch. Environ. Contam. Toxicol.*, **50**: 539–544

Mugiya, Y. and N. Watabe 1977 Studies on fish scale formation and resorption II: Effect of estradiol on calcium homeostasis and skeletal tissue resorption in the goldfish, *Carassius auratus*, and the killifish, *Fundulus heteroclitus. Comp. Biochem. Physiol.*, **57A**: 197–202

Redmayne, A. C., J. P. Kim, G. P. Closs and K. A. Hunter 2000 Methyl mercury bioaccumulation in long–finned eels, *Anguilla dieffenbachii*, from three rivers in Otago, New Zealand. *Sci. Total Environ.*, **262**: 37–47

Suzuki, N., C. Eguchi, T. Hirai and Y. Sasayama 1997 Nucleotide sequences of reptile calcitonins: Their high homology to chicken calcitonin. *Zool. Sci.*, **14**: 833–836

Suzuki, N., T. Suzuki and T. Kurokawa 2000 Suppression of osteoclastic activities by calcitonin in the scales of goldfish (freshwater teleost) and nibbler fish (seawater teleost). *Peptides* **21**: 115–124

Suzuki, N. and A. Hattori 2002 Melatonin suppresses osteoclastic and osteoblastic activities in the scales of goldfish. *J. Pineal Res.*, **33**: 253–258

Suzuki, N. and A. Hattori 2003 Bisphenol A suppresses osteoclastic and osteoblastic activities in the cultured scales of goldfish. *Life Sci.*, **73**: 2237–2247

Suzuki, N., M. Yamamoto, K. Watanabe, A. Kambegawa and A. Hattori 2004 Both mercury and cadmium directly influence calcium homeostasis resulting from the suppression of scale bone cells: The scale is a good model for the evaluation of heavy metals in bone metabolism. *J. Bone Miner. Metab.*, **22**: 439–446

Suzuki, N., M. J. Tabata, A. Kambegawa, A. K. Srivastav, A. Shimada, H. Takeda, M. Kobayashi, S. Wada, T. Katsumata and A. Hattori 2006 Tributyltin inhibits osteoblastic activity and disrupts calcium metabolism through an increase in plasma calcium and calcitonin levels in teleosts. *Life Sci.*, **78**: 2533–2541

Suzuki, N., K. Kitamura, T. Nemoto, N. Shimizu, S. Wada, T. Kondo, M. J. Tabata, F. Sodeyama, K. Ijiri and A. Hattori 2007 Effect of vibration on osteoblastic and osteoclastic activities: Analysis of bone metabolism using goldfish scale as a model for bone. *Adv. Space Res.*, **40**: 1711–1721

Takeuchi, T., K. Eto, S. Oyanag and H. Miyajima 1978 Ultrastructural changes of human sural nerves in the neuropathy induced by intrauterine methylmercury poisoning (so–called fetal Minamata disease). *Virchows Arch. B Cell Path.*, **27**: 137–154

Takeuchi, T. 1982 Pathology of Minamata disease: With special reference to its pathogenesis. *Acta Pathol. Jpn.*, **32 Suppl 1**: 73–99

Yamada, J. 1961 Studies on the structure and growth of the scales in the goldfish. *Mem. Fac. Fish Hokkaido Univ.*, **9**: 181–226

Yonaga, T., Y. Fujino, R. Tamura, K. Kurabayashi, T. Uraya, K. Aono and K. Yoshimura 1985 Effect of organic and inorganic mercury compounds on the growth of incisor and tibia in rats. *Anat. Anz.*, **159**: 373–383

Yoshikubo, H., N. Suzuki, K. Takemura, M. Hoso, S. Yashima, S. Iwamuro, Y. Takagi, M.J. Tabata and A. Hattori 2005 Osteoblastic activity and estrogenic response in the regenerating scale of goldfish, a good model of osteogenesis. *Life Sci.*, **76**: 2699–2709

Parathyroid hormone 1 (1–34) acts on the scales and involves calcium metabolism in goldfish

Nobuo Suzuki [a,*], Janine A. Danks [b], Yusuke Maruyama [c], Mika Ikegame [d], Yuichi Sasayama [a], Atsuhiko Hattori [c], Masahisa Nakamura [e], Makoto J. Tabata [f], Toshio Yamamoto [d], Ryo Furuya [e], Kiyofumi Saijoh [g], Hiroyuki Mishima [h], Ajai K. Srivastav [i], Yukihiro Furusawa [j], Takashi Kondo [j], Yoshiaki Tabuchi [k], Ichiro Takasaki [k], Vishwajit S. Chowdhury [l], Kazuichi Hayakawa [m], T. John Martin [n]

[a] Noto Marine Laboratory, Institute of Nature and Environmental Technology, Kanazawa University, Housu-gun, Ishikawa 927–0553, Japan
[b] School of Medical Sciences, RMIT University, Bundoora 3083, Australia
[c] Department of Biology, College of Liberal Arts and Sciences, Tokyo Medical and Dental University, Ichikawa, Chiba 272–0827, Japan
[d] Department of Oral Morphology, Graduate School of Medicine, Dentistry and Pharmaceutical Sciences, Okayama University, Okayama, Okayama 700-8525, Japan
[e] Department of Biology, Faculty of Education and Integrated Arts and Sciences, Waseda University, Shinjuku-ku, Tokyo 162–8480, Japan
[f] Biostructural Science, Department of Hard Tissue Engineering, Division of Bio-Matrix, Graduate School of Tokyo Medical and Dental University, Bukyo-ku, Tokyo 113–8549, Japan
[g] Department of Hygiene, School of Medicine, Kanazawa University, Kanazawa, Ishikawa 920–8640, Japan
[h] Kochi Gakuen College, Kochi 780–0955, Japan
[i] Department of Zoology, University of Gorakhpur, Gorakhpur 273009, India
[j] Department of Radiological Sciences, Graduate School of Medicine and Pharmaceutical Sciences, University of Toyama, Sugitani, Toyama 930–0194, Japan
[k] Division of Molecular Genetics Research, Life Science Research Center, University of Toyama, Sugitani, Toyama 930–0194, Japan
[l] Department of Bioresource Sciences, Kyushu University, Fukuoka 812–8581, Japan
[m] Graduate School of Natural Science and Technology, Kanazawa University, Kakuma, Ishikawa 920–1192, Japan
[n] St. Vincent's Institute of Medical Research, 41 Victoria Parade, Fitzroy 3065, Australia

ARTICLE INFO

ABSTRACT

The effect of fugu parathyroid hormone 1 (fugu PTH1) on osteoblasts and osteoclasts in teleosts was examined with an assay system using teleost scale and the following markers: alkaline phosphatase (ALP) for osteo-blasts and tartrate-resistant acid phosphatase (TRAP) for osteoclasts. Synthetic fugu PTH1 (1–34) (100 pg/ml–10 ng/ml) significantly increased ALP activity at 6 h of incubation. High-dose (10 ng/ml) fugu PTH1 significantly increased ALP activity even after 18 h of incubation. In the case of TRAP activity, fugu PTH1 did not change at 6 h of incubation, but fugu PTH1 (100 pg/ml–10 ng/ml) significantly increased TRAP activity at 18 h. Similar results were obtained for human PTH (1–34), but there was an even greater response with fugu PTH1 than with human PTH. In vitro, we demonstrated that both the receptor activator of the NF-κB ligand in osteoblasts and the receptor activator NF-κB mRNA expression in osteoclasts increased significantly by fugu PTH1 treatment. In an in vivo experiment, fugu PTH1 induced hypercalcemia resulted from the increase of both osteoblastic and osteoclastic activities in the scale as well as the decrease of scale calcium contents after fugu PTH1 injection. In addition, an in vitro experiment with intramuscular autotransplanted scale indicated that the ratio of multinucleated osteoclasts/mononucleated osteoclasts in PTH-treated scales was significantly higher than that in the control scales. Thus, we concluded that PTH acts on osteoblasts and osteoclasts in the scales and regulates calcium metabolism in goldfish.

© 2011 Elsevier Inc. All rights reserved.

Introduction

Parathyroid hormone (PTH) increases plasma calcium level in mammals and is secreted from the parathyroid gland in all tetrapods, but not in fish. The first animal to evolve parathyroid glands is the amphibian [1]. Recently, the PTH gene has been discovered in Fugu rubripes, and 80 amino acids of the protein-coding region were determined [2]. Fugu PTH1 as well as human PTH specifically bound to the human parathyroid hormone receptor (PTHR) and promoted cyclic AMP formation in a mammalian cell line [2]. In addition, it was found that zebrafish had two PTHs [3] and that zebrafish PTH1 and zebrafish PTH2 mRNAs and PTH1 protein were detected in the neuromasts of the lateral line and in the central nervous system during embryogenesis [4]. These results suggest that PTH synthesized in the neural tissues has a physiological significant role in teleosts.

The teleost scale is a calcified tissue that contains osteoblasts and osteoclasts [5–7]. The scales are a functional internal calcium reservoir during periods of increased calcium demand, such as sexual maturation and starvation [5,7–11]. In the scale, as in mammalian bone, type I collagen [12], bone γ-carboxyglutamic acid protein [13], osteonectin [14,15], and hydroxyapatite [16] are present. Thus, the teleost scale has a number of features in common with mammalian membranous bone.

Recently, we developed a new *in vitro* assay system using fish scale [17,18], which can be used to detect the activities of scale osteoblasts and osteoclasts simultaneously using the alkaline phosphatase (ALP) and the tartrate-resistant acid phosphatase (TRAP) assay, respectively. This assay is an original assay system to detect the respective enzyme activity from a single scale by transferring each scale to a 96-well microplate. These markers (TRAP and ALP) have been shown to be affected by a number of hormones and other factors in osteoclasts and osteoblasts [19–21] in mammals. In the scales of carp, de Vrieze et al. [22] also demonstrated that ALP and TRAP are valid markers for osteoblasts and osteoclasts, respectively.

Using this system, we demonstrated that calcitonin suppressed osteoclastic activity in scale osteoclasts as it does in mammalian osteoclasts [17]. Moreover, we were the first to find that melatonin, a major hormonal product of the pineal gland, functioned negatively in both osteoclasts and osteoblasts [18]. The action of melatonin on bone has also subsequently been reported in *in vivo* studies in the rat [23]. Moreover, we indicated that osteogenesis in the regenerating scale is very similar to that seen in mammalian membranous bone and that regenerating scales have estrogen receptors which respond to estrogen in the same manner as mammalian osteoblasts [24]. Persson et al [25] reported that estrogen specific binding was detected in the scales of rainbow trout. We suggest that this fish scale culture system is useful for the evaluation of the effect of PTH on bone.

In the present study, we examined the effect of fugu PTH1 on goldfish scale osteoblastic and osteoclastic activities and compared the actions of fugu PTH1 with those of human PTH. To confirm the effect of fugu PTH1 on plasma calcium and the scale (osteoblasts and osteoclasts), *in vivo* experiments were carried out. In teleosts, three types of receptors for PTH have been identified [26] and it has been reported that zebrafish PTH1 binds to both PTH1R and PTH3R [3]. In order to confirm that PTH's action on the scales of goldfish was *via* the PTH receptors, we established their presence in the scales by reverse transcription-polymerase chain reaction (RT-PCR) with primers based on the conserved regions for both mammalian and zebrafish PTHR sequences. In addition, expression analyses of both the receptor activator of NF-κB (RANK) and the receptor activator of the NF-κB ligand (RANKL) in the fugu PTH1-treated scales were performed because the RANK–RANKL pathway is necessary for osteoclast differentiation [27–29]. Moreover, the induction of mononucleated osteoclasts to multinucleated osteoclasts was investigated using goldfish scales autotransplanted to muscle.

Materials and methods

Animals

A previous study [17] indicated that the sensitivity for calcemic hormones was higher in mature female than in mature male teleosts. Therefore, female goldfish (*Carassius auratus*) (30–40 g) were purchased and used for all of the *in vitro* experiments and mRNA expression analyses. To examine the effect of fugu PTH1 on the calcium metabolism, immature goldfish (4–6 g), in which the endogenous effects of sex steroids are negligible, were used for the *in vivo* study.

All experimental procedures were conducted in accordance with the Guide for the Care and Use of Laboratory Animals prepared by Kanazawa University.

Effects of fugu PTH1 (1–34) and human PTH (1–34) on ALP and TRAP activities in the cultured scales of goldfish

A 1% penicillin–streptomycin mixture (ICN Biomedicals Inc., OH, USA) was added to Eagle's modified minimum essential medium (MEM; ICN Biomedicals, Inc.). HEPES (Research Organics Inc., OH, USA) (20 mM) was added to MEM and adjusted to pH 7.0. After filtration, MEM was used in the experiments. Scales were collected from goldfish under anesthesia with ethyl 3-aminobenzoate, methanesulfonic acid salt (Sigma-Aldrich, Inc., MO, USA) and incubated for 6 and 18 h in MEM supplemented with: 1) fugu PTH1 (1–34) (1 pg/ml–10 ng/ml); 2) human PTH (1–34) (Bachem AG, Bubendorf, Switzerland) (1 pg/ml– 10 ng/ml); 3) a PTH-free medium as a control. Fugu PTH1 synthesis was carried out as described previously [2]. After incubation, ALP and TRAP activities were measured using the same methods described in Suzuki and Hattori [18]. The results are shown as means ± SEM ($n = 8$). The value of EC50 was calculated using SigmaPlot software (Systat Software Inc.).

Effects of fugu PTH1 (1–34) on scale ALP and TRAP activities, plasma calcium level, and scale calcium content in the goldfish (in vivo experiment)

In the experimental group, goldfish (body weight: 4–7 g) were anesthetized in the same manner as above and then fugu PTH1 (500 ng/g body weight) was injected intraperitoneally. The goldfish in the control group were injected with saline (0.9% NaCl) in the same manner as experimental goldfish. These goldfish were kept in the aquarium for 1, 2, 3, and 4 days (each $n = 10$). During the experimental periods, these goldfish were fasted to exclude intestinal calcium uptake from diets. Each day after injection, blood samples were collected from the gill using a heparinized capillary from individual, anesthetized goldfish. After centrifugation at 15,000 rpm for 3 min, the plasma was immediately frozen and kept at −80 °C until use. The plasma total calcium level (mM) was determined using an assay kit (Calcium C, Wako Pure Chemical Industries, Ltd., Osaka, Japan). At the highest plasma calcium level in goldfish after PTH injection, we measured the ALP and TRAP activity and calcium content in the scale. The scale calcium content (milligram per dry weight (mg) of scale) was determined using the Calcium C kit (Wako) after the scale was dissolved in nitric acid and then neutralized by NaOH.

Cloning of PTHR cDNA from the goldfish scales by RT-PCR

Total RNA was prepared from goldfish scales using a total RNA isolation kit (Nippon Gene, Tokyo, Japan). RT-PCR was performed using Oligotex-dT 30 Super (Takara Bio, Inc., Otsu, Japan) as an oligo dT primer to prevent genomic DNA contamination [30]. The primers were designed on the basis of mammalian PTHRs (mouse PTH1R: P41593; mouse PTH2R: Q91V95; human PTH1R: NP_000307; human PTH2R: NP_005039); and zebrafish (PTH1R: AF132084; PTH2R: AF132082; PTH3R: AF132085). The primer sequences were sense-1: 5′-TAYRTNTAYGAYTTYAAYCAY-3′; sense-2: 5′-CAYTGYACNMG-NAAYTAYATHCAY-3′; antisense-1: 5′-GYYTGNACYTCNCCRTTRCA-3′; and antisense-2: 5′-ACYTCNCCRTTRCARWARCARTA-3′. The first and second PCR (first PCR: sense-1/antisense-1 primer set; second PCR sense-2/antisense-2 primer set) were performed using Taq polymerase (Nippon Gene). The PCR parameters were 35 cycles of denaturation for 0.5 min at 96 °C, annealing for 1 min at 45 °C, and extension for 2 min at 72 °C, followed by a single cycle at 72 °C for 30 min. PCR products obtained by the nested PCR were gel-purified and cloned into pT7blue-T vector (EMD Biosciences, Inc., Novagen Brand, WI, USA). Inserts were sequenced by an automated DNA sequencer (3100 type, Applied Biosystems, CA, USA).

Comparison of PTH1R and PTH2R mRNA expression in the scales

Total RNA was prepared from goldfish scales using a total RNA isolation kit for fibrous tissue and complementary DNA synthesis was performed (RNase Easy Fibrous Mini-Kit, Qiagen GmbH, Hilden, Germany). The PCR amplification was analyzed with a real-time PCR apparatus (Mx3000p™, Stratagene, CA, USA) using the primers for PTH1R (sense: 5′-GCCACTCTTGCTGACACCGAGT-3′; antisense: 5′-ATCTGGATTTGCCACGGCACCC-3′) and for PTH2R (sense: 5′-GGCAACGCTGGCGGATGTAA-3′; antisense: 5′-TGTGTCGTATCGCCCCG-CAT-3′). The annealing temperature of PTH1R and PTH2R was 60 °C. The detailed conditions of PCR were described in our previous study [31].

To confirm the expression level of PTH1R and PTH2R in the goldfish scales, we used a different method in which the PCR conditions for each receptor cDNA would be specifically amplified using the primers for PTH1R (sense: 5′-AATGGAGAGCATCACTGTG-GAAG-3′; antisense: 5′-ACGGCACCCAGACACTTCT-3′) and for PTH2R (sense: 5′-CAACATCAGCACCGTCTCCATT-3′; antisense: 5′-CCCAGGC-CAGACCTGTGAA-3′). Amplification of β-actin cDNA used the primer set: sense: 5′-CACTGTGCCCATCTACGAG-3′; antisense: 5′-CCATCTCC-TGCTCGAAGTC-3′ [32]. The conditions for PCR amplification were denaturation for 0.5 min at 96 °C, annealing for 1 min at 60 °C, and extension for 2 min at 72 °C followed by a single cycle at 72 °C for 30 min. The PCR products were analyzed on a 2.5% NuSive GTG agarose gel (FMC BioProducts, ME, USA) and stained with ethidium bromide. The band densities were estimated using a computer program (NIH Image J).

Expression analyses of RANK and RANKL mRNAs in fugu PTH1 (1–34)-treated scales

Scales collected from goldfish under anesthesia as described above and incubated for 6 and 18 h in MEM supplemented with fugu PTH1 (10 ng/ml) and a PTH-free medium as a control. After incubation, the scales were immediately frozen and kept at −80 °C until use.

Total RNA was prepared from goldfish scales using the method set out above and complementary DNA was synthesized. The primers (RANK-sense:5′-AAGTGGACAGATTGTAAAGCTAT-3′; RANK-antisense: 5′-GCCACCTGATGAGGTTTCAGCAC-3′; RANKL-sense: 5′-GCGCT-TACCTGCGGAATCATATC-3′; RANKL-antisense: 5′-AAGTGCAACA-GAATCGCCACAC-3′) were designed using the zebrafish RANK sequence (Accession no. XM_001918948) and the RANKL sequence in goldfish (Accession no. AB459540). The PCR amplification was analyzed by a real-time PCR apparatus (Stratagene). Amplification of β-actin was performed using primers (sense: 5′-CGAGCGTGGCTA-CAGCTTCA-3′ ; antisense: 5′-GCCCGTCAGGGAGCTCATAG-3′) [33]. The PCR amplification was analyzed by real-time PCR. The detailed conditions of PCR were described in our previous study [31]. The annealing temperature of RANK, RANKL, and β-actin was 60 °C. The RANK and RANKL mRNA levels were normalized to the β-actin mRNA level.

Effect of fugu PTH1(1–34) on the differentiation of mononucleated osteoclasts into multinucleated osteoclasts using the intramuscular autotransplanted scales

Goldfish were anesthetized and to induce mononucleated osteo-clasts into the surface of the scale, the scales collected from goldfish were intramuscularly autotransplanted [34]. Thereafter, the goldfish were kept in tap water containing an antibiotic (Green F Gold, Sanei Co., Ltd., Tokyo, Japan) at 25 °C for 3 days. The goldfish were again anesthetized. The implanted scales were taken out and cut into two pieces. The half was put into each well of a microplate and pre-incubated with MEM for 6 h. One piece of scale was then incubated with fugu PTH1 (10 ng/ml), and the other piece was incubated without hormone. After the incubation, the pieces of the scales were fixed in 10% formalin in a 0.05 M cacodylate buffer (pH 7.4). TRAP

staining of the scales was performed by the methods of Cole and Walters [35]. After TRAP staining, the specimens were counterstained with 4′, 6-diamino-2-phenylindole (DAPI) (Molecular Probes, Inc., Eugene, OR, USA). Then, the numbers of mono- and multinucleated osteoclasts were counted.

To examine the fine structure of multinucleated osteoclasts, the fugu PTH1-treated scales were fixed with 2.5% glutaraldehyde (Nacalai Tesque, Inc., Kyoto, Japan) in a 0.1 M cacodylate buffer at pH 7.4 for 1 h. After fixation, the specimens were decalcified with 5% EDTA for 3 days. Following post-fixation with 1% osmium tetroxide (Merck KGaA, Darmstadt, Germany), the specimens were dehydrated and embedded in Epon 812 (TAAB Laboratories, Berks, U.K.). Ultrathin sections were obtained from the Epon blocks and stained with uranyl acetate and lead citrate. These sections were observed under an electron microscope (H-500, Hitachi, Tokyo, Japan) operated at 100 kV.

Statistical analysis

In the experiments involving RT-PCR and osteoclast differentiation with intramuscular autotransplanted scale, the data were analyzed using the paired *t*-test. In other experiments, statistical significance was analyzed by one- or two-way ANOVA followed by the Dunnett test. The significance level was $P<0.05$.

Results

Effects of fugu PTH1 (1–34) and human PTH (1–34) on ALP and TRAP activities in the cultured scales of goldfish

Fugu PTH1 (100 pg/ml–10 ng/ml) significantly increased ALP activity in 6 h incubations (Fig. 1A). After 18 h of incubation, the ALP activity remained significantly increased only at 10 ng/ml (Fig. 1B).

ALP activity was also increased by human PTH with 6 h of incu-bation; however, by two-way ANOVA analysis, there was a signifi-cantly greater ($P<0.05$) response with fugu PTH1 than with human PTH at 6 h of incubation (Fig. 1A). The EC50 values of fugu PTH1 and human PTH were 18 and 76 (pg/ml), respectively. After 18 h of incu-bation, the activation of ALP remained high only at the 10 ng/ml dose of both fugu PTH1 and human PTH (Fig. 1B).

Neither fugu nor human PTH treatment altered TRAP activity after 6 h incubation (Fig. 2A), but, at 18 h TRAP activity increased in scales treated with either PTH (Fig. 2B), with fugu PTH1 being more potent than human PTH.

Effects of fugu PTH1 (1–34) on scale ALP and TRAP activities, plasma calcium level, and scale calcium content in the goldfish (in vivo experiment)

After a single injection of fugu PTH1 into immature goldfish, the plasma calcium level increased for 1–3 days, with the highest level at day 2 after injection (Fig. 3A). At that time, the scale calcium content was decreased significantly (Fig. 3B), and both ALP and TRAP activities in the scale were significantly increased (Fig. 3C and D).

Partial amino acid sequences of goldfish PTHRs

Sequence analysis indicated that there were two different cDNA fragments amplified. One fragment had a high degree (96.6%) of amino acid identity to zebrafish PTH1R (AF132084), while the identity of the other fragment to zebrafish PTH2R (AF132082) was 84.8%. The amino acid sequence identity of both fragments to zebrafish PTHR3 (AF132085) was 60.3% and 50.0%, respectively. Therefore, it was concluded that these goldfish fragments are goldfish PTH1R (AB497045) and PTH2R (AB497046), respectively.
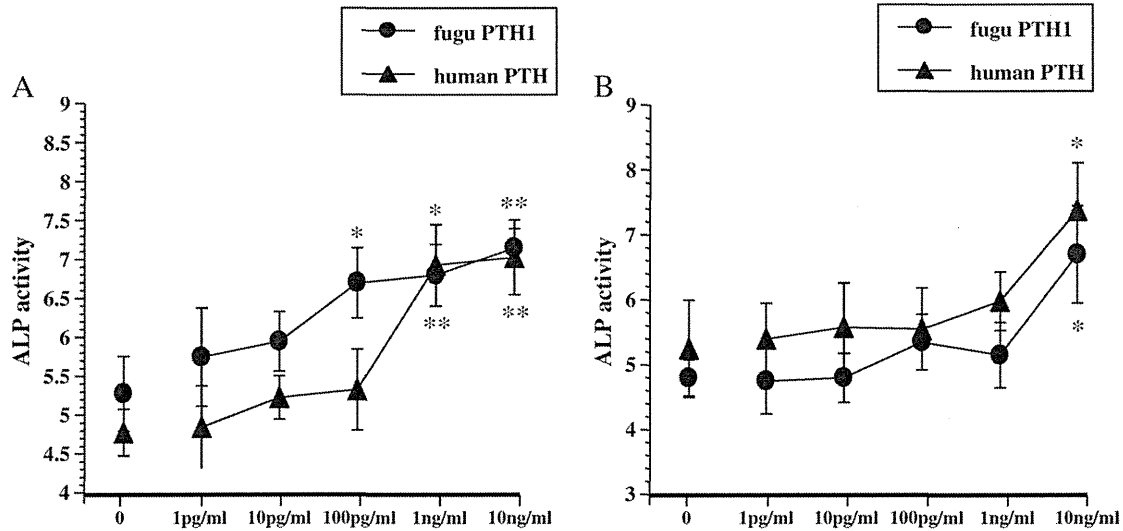
Fig. 1. Effects of fugu PTH1 and human PTH on ALP activity in cultured goldfish scales after 6 h (A) and 18 h (B) of incubation. * and ** indicate statistically significant differences at $P<0.05$ and $P<0.01$, respectively, from the values in the control scales. ALP activity was calculated as nanomole pNP produced per milligram scale per hour $(n=8)$.

### Comparison of PTH1R and PTH2R mRNA expressions in the scales

Since it appeared from semi-quantitative PCR that PTH1R was more abundant than PTH2R, we carried out quantitative RT-PCR. The band strength of RT-PCR indicated that expression of PTH1R mRNA in the scale was greater than that of PTH2R mRNA (Fig. 4).

### Expression analyses of RANK and RANKL mRNAs in fugu PTH1 (1–34)-treated scales

Fig. 5 shows RANK and RANKL mRNA expression with and without fugu PTH1 treatment. After 6 h incubation of goldfish scales *in vitro*, RANK mRNA expression in fugu PTH-treated scales was significantly increased compared with control (Fig. 5), and this difference was further enhanced at the 18 h incubation time point. RANKL mRNA expression in the PTH-treated scales increased significantly and to approximately the same extent at both 6 and 18 h of incubation.

Effect of fugu PTH1 (1–34) on the differentiation of mononucleated osteoclasts into multinucleated osteoclasts using the intramuscular autotransplanted scales

Mononucleated osteoclasts were induced on the surface of the scales at 3 days after intramuscular autotransplantation of the goldfish scales. Using these scales, an *in vitro* experiment was performed. After 24 and 48 h of incubation, the ratio of multinucleated osteoclasts/mononucleated osteoclasts in PTH-treated scales was significantly higher than that in the control scales (Fig. 6A). The number of mono- and multinucleated osteoclasts in the fugu PTH1-treated scales was significantly higher than that in the control scales at both 24 and 48 h (Fig. 6B). Results of TRAP staining in the PTH-treated scale and control scale are indicated in Fig. 7. The edges of the PTH-treated scale were strongly stained by TRAP. Typical mono- and multi-nucleated osteoclasts in the edges of the scales are indicated in Fig. 8. In addition, the fine structure of the multinucleated osteoclasts is shown in Fig. 9. The multinucleated osteoclasts had several nuclei,
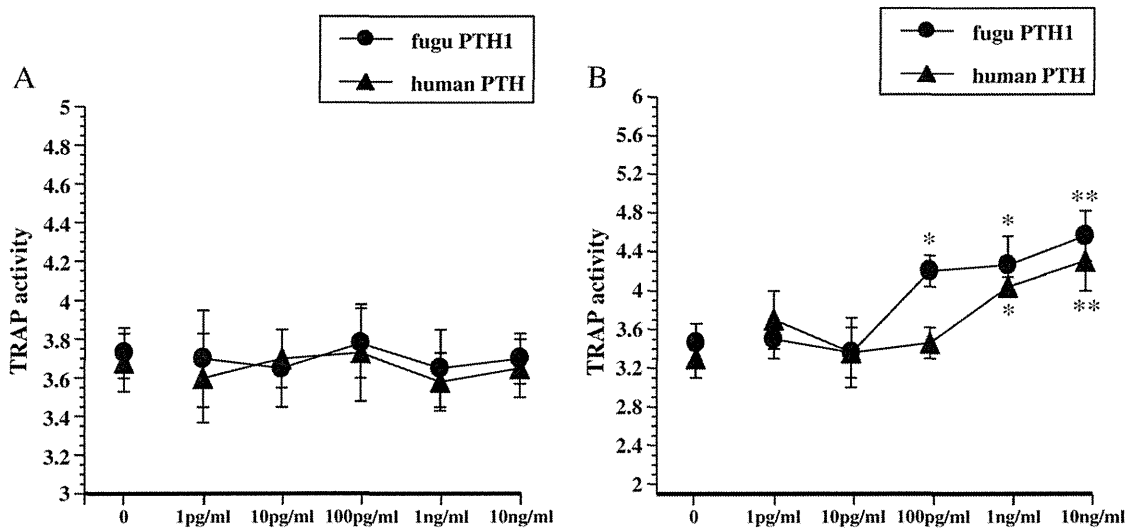
Fig. 2. Effects of fugu PTH1 and human PTH on TRAP activity in cultured goldfish scales after 6 h (A) and 18 h (B) of incubation. * and ** indicate statistically significant differences at $P<0.05$ and $P<0.01$, respectively, from the values in the control scales. TRAP activity was calculated as nanomole pNP produced per milligram scale per hour $(n=8)$.
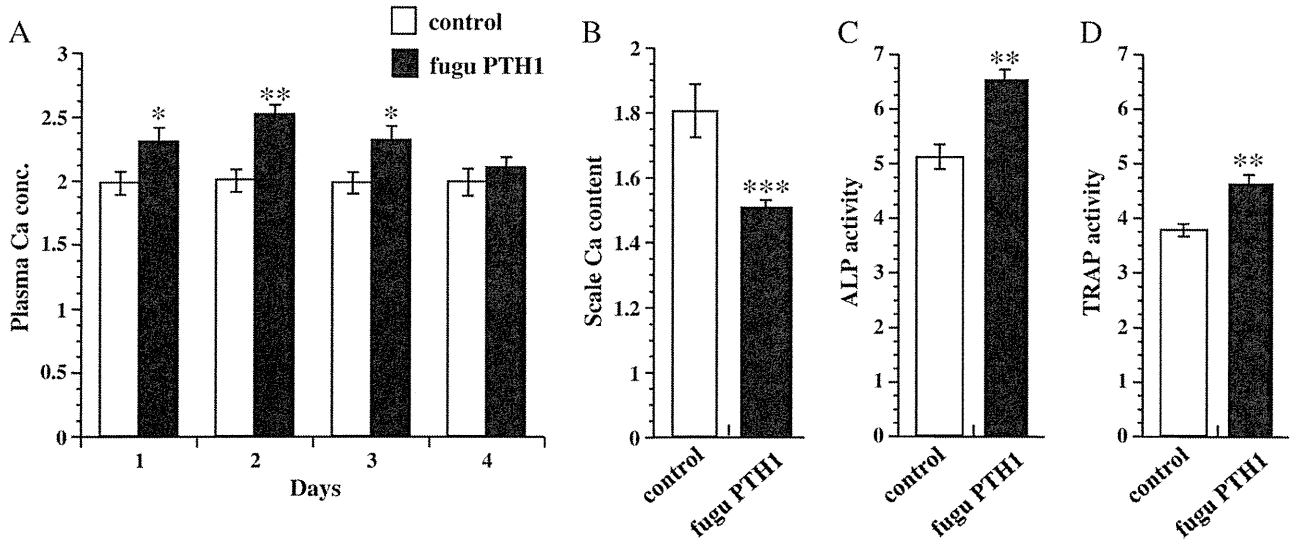
Fig. 3. Effects of fugu PTH1 on plasma calcium (mM) (A), scale calcium content (milligram per dry weight (mg) of scale) (B), scale ALP (C) and TRAP (D) activities (nanomole pNP produced per milligram scale per hour) in an *in vivo* experiment using immature goldfish. *, **, and *** indicate statistically significant differences at $P<0.05$, $P<0.01$, and $P<0.001$, respectively, from the values in the control. The graph shows the means ± SEM ($n=10$).

a ruffled border, a clear zone, abundant mitochondria, and perinuclear Golgi complexes and were very similar to the mammalian multinucleated osteoclasts.

Discussion

Using an *in vitro* assay system with goldfish scales, we have shown that fugu PTH1 (1–34) increased both ALP and TRAP activities in the scales. The *in vitro* data were supported by our *in vivo* findings, in which hypercalcemia was induced by fugu PTH and was associated with a decline of scale calcium content, consistent with mobilization of scale calcium. In addition, we have shown that the ratio of multinucleated osteoclasts/mononucleated osteoclasts in PTH-treated scales was significantly higher than that in the control scales using intramuscular autotransplanted scales *in vitro*. The osteoclasts in the goldfish scale were found to be almost identical to mammalian osteoclasts, judging from their electron microscopic appearance. In teleosts, thus, PTH appears to act directly on the scales and may influence the plasma calcium level through those cellular actions, as is the case in mammalian bone.

In the reproductive period of female teleosts, the plasma calcium level increases remarkably [36–38]. This calcium is bound to vitellogenin, which is a major component of egg protein and a calcium-binding protein [39,40]. In this period, calcitonin, which has a hypocalcemic action through inhibiting scale osteoclasts, plays an important role. In fact, the plasma calcitonin level of female teleost increases in the reproductive period [38,41]. Using an *in vitro* assay system, we found that goldfish calcitonin suppressed osteoclastic activity in the goldfish scales [17]. In our present *in vivo* study, hypercalcemia was induced by fugu PTH1 injection. In the vitellogenesis of female teleosts, we believe that PTH functions to remove calcium from the scales. However, there is no data concerning the involvement of PTH in bone metabolism in fish during reproductive seasons. Further work to follow up this study will include examining PTH and PTHR mRNA expressions in the scales during reproduction, and, thereby, elucidating the physiological role of PTH in teleosts.

In mammals, RANKL produced by cells in the osteoblast lineage binds to RANK in mononuclear hemopoietic precursors and promotes
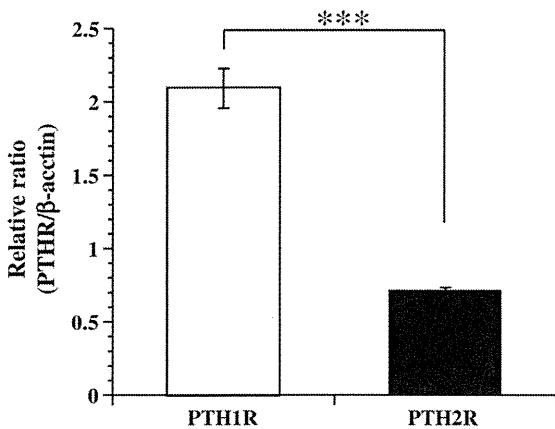

Fig. 4. Comparison of PTH1R and PTH2R mRNA expressions in goldfish scales. In the RT-PCR analysis, the PTH1R and PTH2R mRNA levels were normalized to the β-actin mRNA level ($n=8$). *** indicates statistically significant difference at P<0.001 between the values of PTH1R and PTH2R.
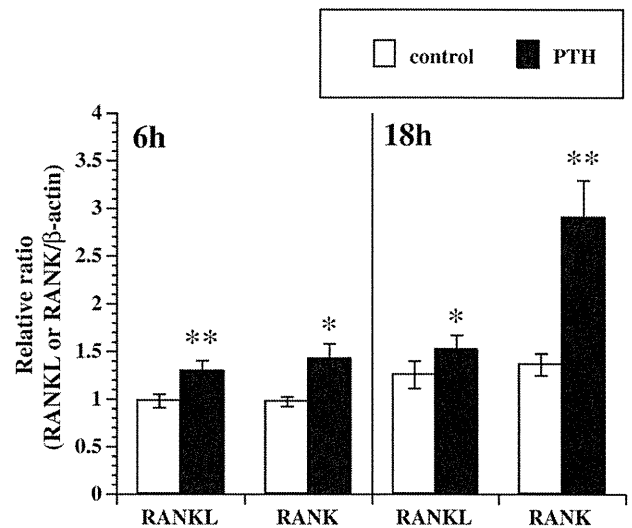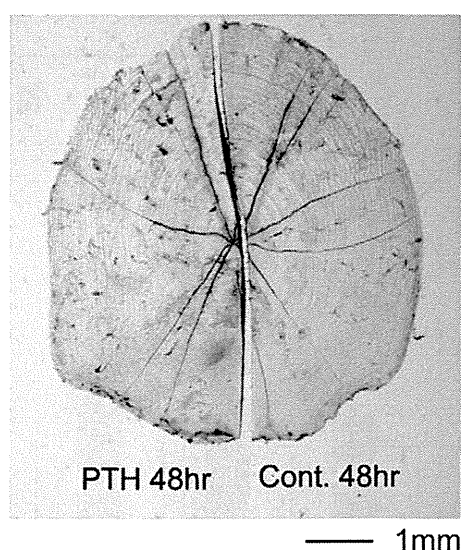

Fig. 5. Expression analysis of RANK and RANKL mRNAs in the fugu PTH1 (10 ng/ml)-treated scale. The RANK and RANKL mRNA levels were normalized to the β-actin mRNA level. * and ** indicate statistically significant differences at $P<0.05$ and $P<0.01$, respectively, from the values in the control scales ($n=8$).
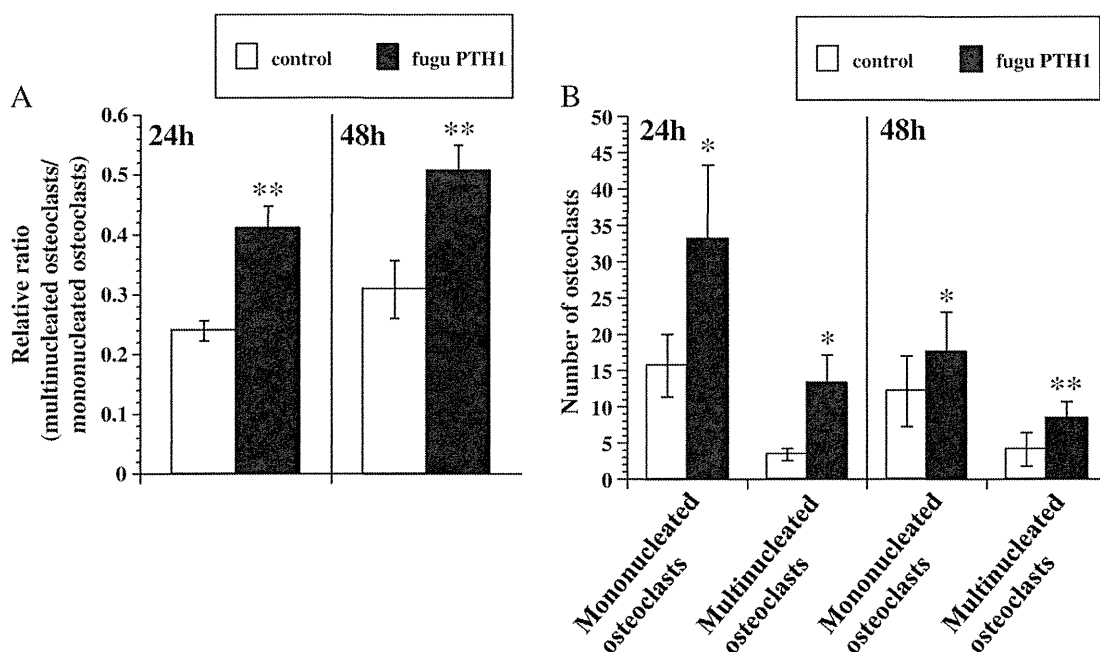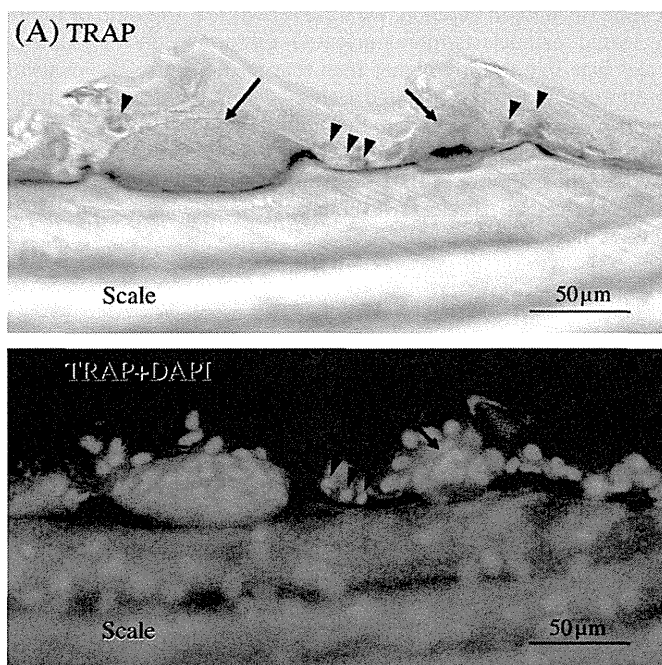
Fig. 6. Relative ratio of multinucleated osteoclasts/mononucleated osteoclasts (A) and number of mono- and multinucleated osteoclasts (B) in the fugu PTH1-treated scales. At 3 days after intramuscular autotransplantation, the scales were removed and cut into half. After pre-incubation with a PTH-free culture medium for 6 h, one half of the scale was cultured for 24 and 48 h with fugu PTH1 (10 ng/ml) and then fixed and stained for TRAP. The other half was cultured for 24 and 48 h without fugu PTH1 and then fixed and stained for TRAP. After 4',6-diamino-2-phenylindole (DAPI) staining, the number of mono- and multinucleated osteoclasts was counted. * and ** indicate statistically significant differences at $P<0.05$ and $P<0.01$, respectively, from the values in the control scales ($n=8$).

the formation and activity of multinucleated osteoclasts [27]. In mammals, PTH1R is located in the osteoblast lineage and increases osteoclastic formation and activity via the RANK–RANKL pathway [27–29]. Our present data demonstrates that fugu PTH1 can increase osteoblastic activity and then activate osteoclasts in the goldfish scale. The increased RANKL mRNA in response to PTH treatment in scales (Fig. 5) most likely reflects an action of PTH on the osteoblasts of scales whereas the increased RANK production is the result of increased osteoclast generation, as confirmed in Figs 6–9. Since PTH1R is mainly expressed in the scale, this hormone seems likely to bind to PTH1R in osteoblasts as well as in mammals.

In the present study, we cloned both PTH1R and PTH2R cDNAs from the goldfish scales and found a greater abundance of PTH1R than PTH2R. A ligand of PTH2R is a tuberoinfundibular peptide (TIP) isolated from bovine hypothalamus [42,43]. As both TIP and PTH2R are strongly expressed in the hypothalamus, it was considered that TIP acts on the nervous system in mammals [43,44]. In tilapia,

Fig. 7. The whole mount TRAP staining of the intramuscular autotransplanted scale. At 3 days after intramuscular autotransplantation, the scales were removed and bisected. After pre-incubation with a PTH-free culture medium for 6 h, one half of the scale was cultured for 48 h with fugu PTH1 (10 ng/ml) and the other half was cultured for 48 h without fugu PTH1. Both halves were fixed and stained for TRAP.

Fig. 8. Microscopic views of autotransplanted scales stained for TRAP (A) and TRAP-DAPI (B). At 3 days after intramuscular autotransplantation, the scales were removed and bisected. After pre-incubation with a PTH-free culture medium for 6 h, one half of the scales were cultured for 48 h with fugu PTH1 (10 ng/ml) and subsequently fixed and stained for TRAP and counterstained with 4',6-diamino-2-phenylindole (DAPI). Arrow heads: mononucleated osteoclasts. Arrows: multinucleated osteoclasts.
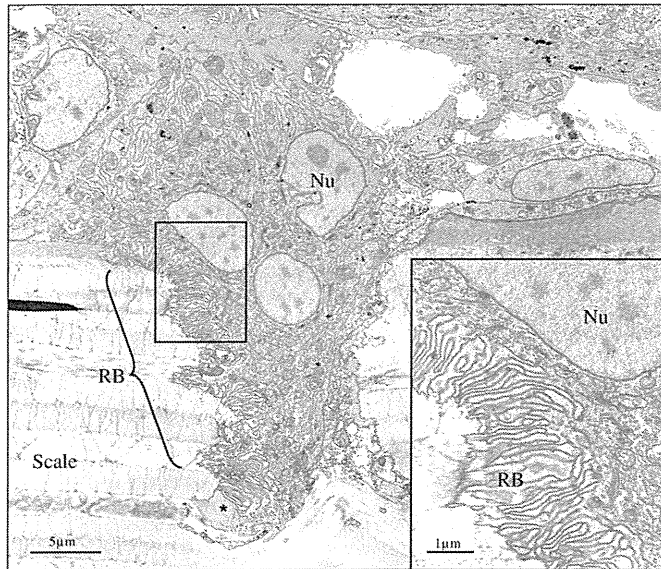
Fig. 9. Fine structure of a multinucleated osteoclast in the fugu PTH1-treated scales. At 3 days after intramuscular autotransplantation, the intramuscular autotransplanted scales were removed and cut into half. After pre-incubation with a PTH-free culture medium for 6 h, one half of the scale cultured for 48 h with fugu PTH1 (10 ng/ml) was then fixed and observed using electron microscopy. The inset is a higher magnification of the square. Nu: nucleus, RB: ruffled border, asterisk (*): clear zone.

however, TIP mRNA was expressed in excretory organs, such as the gill and kidney [45]. In addition, the expression of TIP mRNA in the gill and kidney of seawater-acclimated fish was higher than that of freshwater-acclimated fish, suggesting that the TIP as well as PTH influences the mineral metabolism in teleosts.

Rotllant et al. [46] found that the parathyroid hormone-related protein increased osteoclastic activity in seawater fish scales via cAMP/AC, and Canario et al. [47] found that PTH1 or PTH2 failed to activate the cAMP/AC pathway or stimulate calcium transport in seawater fish scales. Notwithstanding these differences, it is known that the exchange of calcium in the scales of freshwater teleosts is faster than that in marine teleosts because freshwater teleosts live in a low-calcium environment. In fact, the response of estrogen and calcitonin in the scales of freshwater teleosts was higher than that in those of marine teleosts [17,48–50]. In a freshwater teleost, such as goldfish, we can clearly show dose-dependent effects of PTH on osteoblastic and osteoclastic parameters in vitro, and effects of PTH on scale and plasma calcium in vivo. Therefore, further studies are needed to elucidate the signaling pathway and physiological role of PTH in the scale.

In teleosts, plasma PTH level has not yet been measured by homologous assay. In trout and goldfish, plasma PTH levels have been detected by heterologous RIA system with bovine PTH (1–84) antibody. The plasma level of goldfish was around 1.5 (ng/ml) [51]. This might indicate that plasma level of PTH in goldfish is at least one order of magnitude higher than in mammals, but specific, homologous assays will be needed to establish this. In the future, we will determine the PTH sequence in goldfish and develop specific antibody to measure the plasma level of PTH in goldfish.

We recently sequenced osteocalcin from goldfish scales. Using this sequence, we preliminarily examined the effect of PTH on osteoblasts by real-time PCR method. We found that the mRNA expression of osteocalcin in PTH-treated scales was twice higher than that in control scales. We strongly believe that the action of PTH on scale osteoblasts is direct, and most likely indirect on scale osteoclasts, and resemble those in mammalian bone. In addition, we are planning for future experiment with prelabeling mononucleated-osteoclasts or transgenetic mononucleated-osteoclasts to demonstrate the differentiation from mononucleated-osteoclasts to multinucleated-osteoclasts.

In the past, our laboratory has sequenced TRAP and cathepsin K from the goldfish scale [33]. In the scale osteoclasts, the osteoclast markers TRAP and cathepsin K were expressed which were detected by in situ hybridization [33]. In osteoblasts as well, type I collagen [12], osteocalcin [13], and osteonectin [14,15] are present in the scales. In fact, it was reported that teleost scale was more important in these animals as a store of calcium than vertebra, jaw, and otolith, judging from the study of $^{45}Ca^{2+}$-prelabeled scale, vertebra, jaw, and otolith of goldfish and killifish [9]. Considering these facts together with the present study, we conclude that the teleost scale is a functional calcium source analogous to the skeleton in mammals.

Acknowledgments

References

[1] Guerreiro PM, Renfro JL, Power DM, Canario AVM. The parathyroid hormone family of peptides: structure, tissue distribution, regulation, and potential functional roles in calcium and phosphate balance in fish. Am J Physiol Regul Integr Comp Physiol 2007;292:R679–96.
[2] Danks JA, Ho PM, Notini AJ, Katsis F, Hoffmann P, Kemp BE, et al. Identification of a parathyroid hormone in the fish Fugu rubripes. J Bone Miner Res 2003;18: 1326–31.
[3] Gensure RC, Ponugoti B, Gunes Y, Papasani MR, Lanske B, Bastepe M, et al. Identification and characterization of two parathyroid hormone-like molecules in zebrafish. Endocrinology 2004;145:1634–9.
[4] Hogan BM, Danks JA, Layton JE, Hall NE, Heath JK, Lieschke GJ. Duplicate zebrafish pth genes are expressed along the lateral line and in the central nervous system during embryogenesis. Endocrinology 2005;146:547–51.
[5] Yamada J. Studies on the structure and growth of the scales in the goldfish. Mem Fac Fish Hokkaido Univ 1961;9:181–226.
[6] Yamada J. A fine structural aspect of the development of scales in the chum salmon fry. Bull Japan Soc Sci Fish 1971;37:18–29.
[7] Bereiter-Hahn J, Zylberberg L. Regeneration of teleost fish scale. Comp Biochem Physiol 1993;105A:625–41.
[8] Berg A. Studies on the metabolism of calcium and strontium in freshwater fish. I. Relative contribution of direct and intestinal absorption. Mem Ist Ital Idrobiol 1968;23:161–96.
[9] Mugiya Y, Watabe N. Studies on fish scale formation and resorption II: effect of estradiol on calcium homeostasis and skeletal tissue resorption in the goldfish, Carassius auratus, and the killifish, Fundulus heteroclitus. Comp Biochem Physiol 1977;57A:197–202.
[10] Takagi Y, Hirano T, Yamada J. Scale regeneration of tilapia (Oreochromis niloticus) under various ambient and dietary calcium concentrations. Comp Biochem Physiol 1989;92A:605–8.
[11] Persson P, Sundell K, Björnsson BTh, Lundqvist H. Calcium metabolism and osmoregulation during sexual maturation of river running Atlantic salmon. J Fish Biol 1998;52:334–49.
[12] Zylberberg L, Bonaventure J, Cohen-Solal L, Hartmann DJ, Bereiter-Hahn J. Organization and characterization of fibrillar collagens in fish scales in situ and in vitro. J Cell Sci 1992;103:273–85.
[13] Nishimoto SK, Araki N, Robinson FD, Waite JH. Discovery of bone γ-carboxyglutamic acid protein in mineralized scales. J Biol Chem 1992;267:11600–5.
[14] Lehane DB, McKie N, Russell RGG, Henderson IW. Cloning of a fragment of the osteonectin gene from goldfish, Carassius auratus: its expression and potential regulation by estrogen. Gen Comp Endocrinol 1999;114:80–7.
[15] Redruello B, Estevao MD, Rotllant J, Guerreiro PM, Anjos LI, Canario AVM, et al. Isolation and characterization of piscine osteonectin and down regulation of its expression by PTH-related protein. J Bone Miner Res 2005;20:682–92.
[16] Onozato H, Watabe N. Studies on fish scale formation and resorption III: fine structure and calcification of the fibrillary plates of the scales in Carassius auratus (Cypriniformes: Cyprinidae). Cell Tissue Res 1979;201:409–22.
[17] Suzuki N, Suzuki T, Kurokawa T. Suppression of osteoclastic activities by calcitonin in the scales of goldfish (freshwater teleost) and nibbler fish (seawater teleost). Peptides 2000;21:115–24.

[18] Suzuki N, Hattori A. Melatonin suppresses osteoclastic and osteoblastic activities in the scales of goldfish. J Pineal Res 2002;33:253–8.
[19] Vaes G. Cellular biology and biochemical mechanism of bone resorption. Clin Orthop 1988;231:239–71.
[20] Dimai HP, Linkhart TA, Linkhart SG, Donahue LR, Beamer WG, Rosen CJ, et al. Alkaline phosphatase levels and osteoprogenitor cell numbers suggest bone formation may contribute to peak bone density differences between two inbred strains of mice. Bone 1998;22:211–6.
[21] Suda T, Takahashi N, Udagawa N, Jimi E, Gillespie MT, Martin TJ. Modulation of osteoclast differentiation and function by the new members of the tumor necrosis factor receptor and ligand families. Endocr Rev 1999;20:345–57.
[22] de Vrieze E, Metz JR, Von den Hoff JW, Flik G. ALP, TRAcP and cathepsin K in elasmoid scales: a role in mineral metabolism. J Appl Ichthyol 2010;26:210–3.
[23] Ladizesky MG, Boggio V, Albornoz LE, Castrillón PO, Mautalen C, Cardinali DP. Melatonin increases oestradiol-induced bone formation in ovariectomized rats. J Pineal Res 2003;34:143–51.
[24] Yoshikubo H, Suzuki N, Takemura K, Hoso M, Yashima S, Iwamuro S, et al. Osteoblastic activity and estrogenic response in the regenerating scale of goldfish, a good model of osteogenesis. Life Sci 2005;76:2699–709.
[25] Persson P, Shrimpton JM, McCormick SD, Björnsson BTh. The presence of high-affinity, low-capacity estradiol-17β binding in rainbow trout scale indicates a possible endocrine route for the regulation of scale resorption. Gen Comp Endocrinol 2000;120:35–43.
[26] Rubin DA, Jüppner H. Zebrafish express the common parathyroid hormone/parathyroid hormone-related peptide receptor (PTH1R) and a novel receptor (PTH3R) that is preferentially activated by mammalian and fugufish parathyroid hormone-related peptide. J Biol Chem 1999;274:28185–90.
[27] Teitelbaum SL. Bone resorption by osteoclasts. Science 2000;289:1504–8.
[28] Hofbauer LC, Kühne CA, Viereck V. The OPG/RANKL/RANK system in metabolic bone disease. J Musculoskelet Neuronal Interact 2004;4:268–75.
[29] Gensure RC, Gardella TJ, Jüppner H. Parathyroid hormone and parathyroid hormone-related peptide, and their receptors. Biochem Biophys Res Commun 2005;328:666–78.
[30] Suzuki N, Eguchi C, Hirai T, Sasayama Y. Nucleotide sequences of reptile calcitonins: their high homology to chicken calcitonin. Zool Sci 1997;14:833–6.
[31] Furusawa Y, Tabuchi Y, Takasaki I, Wada S, Ohtsuka K, Kondo T. Gene networks involved in apoptosis induced by hyperthermia in human lymphoma U937 cells. Cell Biol Int 2009;33:1253–62.
[32] Chan K-W, Yu K-L, Rivier J, Chow BK-C. Identification and characterization of a receptor from goldfish specific for a teleost growth hormone-releasing hormone-like peptide. Neuroendocrinology 1998;68:44–56.
[33] Azuma K, Kobayashi M, Nakamura M, Suzuki N, Yashima S, Iwamuro S, et al. Two osteoclastic markers expressed in multinucleate osteoclasts of goldfish scales. Biochem Biophys Res Commun 2007;362:594–600.
[34] Takahashi H, Suzuki N, Takagi C, Ikegame M, Yamamoto T, Takahashi A, et al. Prolactin inhibits osteoclastic activity in the goldfish scale: a novel direct action of prolactin in teleosts. Zool Sci 2008;25:739–45.
[35] Cole AA, Walters LM. Tartrate-resistant acid phosphatase in bone and cartilage following decalcification and cold-embedding in plastic. J Histochem Cytochem 1987;35:203–6.
[36] Watts EG, Copp DH, Deftos LJ. Changes in plasma calcitonin and calcium during the migration of salmon. Endocrinology 1975;96:214–8.
[37] Yamauchi H, Orimo H, Yamauchi K, Takano K, Takahashi H. Increased calcitonin levels during ovarian development in the eel, Anguilla japonica. Gen Comp Endocrinol 1978;36:526–9.
[38] Norberg B, Björnsson BTh, Brown CL, Wichardt U-P, Deftos LJ, Haux C. Changes in plasma vitellogenin, sex steroids, calcitonin, and thyroid hormones related to sexual maturation in female brown trout (Salmo trutta). Gen Comp Endocrinol 1989;75:316–26.
[39] Tinsley D. A comparison of plasma levels of phosphoprotein, total protein and total calcium as indirect indices of exogenous vitellogenesis in the Crucian carp, Carassius carassius (L.). Comp Biochem Physiol 1985;80B:913–6.
[40] Kwon HC, Hayashi S, Mugiya Y. Vitellogenin induction by estradiol-17β in primary hepatocyte culture in the rainbow trout, Oncorhynchus mykiss. Comp Biochem Physiol 1993;104B:381–6.
[41] Suzuki N, Yamamoto K, Sasayama Y, Suzuki T, Kurokawa T, Kambegawa A, et al. Possible direct induction by estrogen of calcitonin secretion from ultimobranchial cells in the goldfish. Gen Comp Endocrinol 2004;138:121–7.
[42] Usdin TB, Hoare SRJ, Wang T, Mezey E, Kowalak JA. TIP39: a new neuropeptide and PTH2-receptor agonist from hypothalamus. Nat Neurosci 1999;2:941–3.
[43] Piserchio A, Usdin TB, Mierke DF. Structure of tuberoinfundibular peptide 39 residues. J Biol Chem 2000;275:27284–90.
[44] Dobolyi A, Palkovits M, Usdin TB. Expression and distribution of tuberoinfundibular peptide of 39 residues in the rat central nervous system. J Comp Neurol 2003;455:547–66.
[45] Shoemaker JM, Riley LG, Hirano T, Grau EG, Rubin DA. Differential expression of tuberoinfundibular peptide 38 and glucose-6-phosphatase in tilapia. Gen Comp Endorinol 2006;146:186–94.
[46] Rotllant J, Redruello B, Guerreio PM, Fernandes H, Canario AVM, Power DM. Calcium mobilization from fish scale is mediated by parathyroid hormone related protein via the parathyroid hormone type 1 receptor. Regul Pept 2005;132:33–40.
[47] Canario AVM, Rotllant J, Fuentes J, Guerreio PM, Teodosio HR, Power DM, et al. Novel bioactive parathyroid hormone and related peptides in teleost fish. FEBS Let 2006;580:291–9.
[48] Persson P, Sundell K, Björnsson BTh. Estradiol-17β-induced calcium uptake and resorption in juvenile rainbow trout, Oncorhynchus mykiss. Fish Physiol Biochem 1994;13:379–86.
[49] Persson P, Takagi Y, Björnsson BTh. Tartrate resistant acid phosphatase as a marker for scale resorption in rainbow trout, Oncorhynchus mykiss: effects of estradiol-17β treatment and refeeding. Fish Physiol Biochem 1995;14:329–39.
[50] Guerreiro PM, Fuentes J, Canario AVM, Power DM. Calcium balance in sea bream (Sparus aurata): the effect of oestradiol-17β. J Endocrinol 2002;173:377–85.
[51] Harvey S, Zeng Y-Y, Pang PKT. Parathyroid hormone-like immunoreactivity in fish plasma and tissues. Gen Comp Endocrinol 1987;68:136–46.
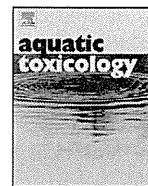
Tributyltin-binding protein type 1, a lipocalin, prevents inhibition of osteoblastic activity by tributyltin in fish scales

Hina Satone[a], Jae Man Lee[b], Yumi Oba[a], Takahiro Kusakabe[b], Eriko Akahoshi[a], Shizuho Miki[a], Nobuo Suzuki[c], Yuichi Sasayama[c], Mohamed Nassef[a], Yohei Shimasaki[a], Shun-ichiro Kawabata[d], Tsuneo Honjo[a], Yuji Oshima[a],*

[a] Laboratory of Marine Environmental Science, Department of Bioscience and Biotechnology, Faculty of Agriculture, Kyushu University, Hakozaki 6-10-1, Higashi-ku, Fukuoka 812-8581, Japan
[b] Laboratory of Silkworm Science, Faculty of Agriculture, Kyushu University, Hakozaki 6-10-1, Higashi-ku, Fukuoka 812-8581, Japan
[c] Noto Marine Laboratory, Institute of Nature and Environmental Technology, Kanazawa University, Noto-cho, Ishikawa 927-0553, Japan
[d] Department of Biology, Faculty of Sciences, Kyushu University, Hakozaki 6-10-1, Higashi-ku, Fukuoka 812-8581, Japan

ARTICLE INFO

ABSTRACT

Tributyltin-binding protein type 1 (TBT-bp1) is a member of the lipocalin family of proteins which bind to small hydrophobic molecules. In this study, we expressed a recombinant TBT-bp1 (rTBT-bp1, ca. 35 kDa) in a baculovirus expression system and purified the protein from the hemolymph of silkworm larvae injected with recombinant baculovirus. After incubation of a mixture of rTBT-bp1 and TBT and its fractionation by means of gel filtration chromatography, TBT was detected in the elution peak of rTBT-bp1, confirming the binding potential of rTBT-bp1 for TBT. An assay of the ability of rTBT-bp1 or native TBT-bp1 (nTBT-bp1) to restore osteoblastic activity inhibited by TBT showed that co-treatment of the scales with rTBT-bp1 or nTBT-bp1 in combination with TBT restored osteoblastic activity in goldfish scales, whereas treatment with TBT alone significantly inhibited osteoblastic activity. These results suggest that TBT-bp1 as a lipocalin member might function to decrease the toxicity of TBT by binding to TBT.

© 2011 Elsevier B.V. All rights reserved.

1. Introduction

The lipocalins are a large family of small extracellular proteins that bind to small endogenous or exogenous hydrophobic molecules such as retinol or drugs and play roles in the immune response and other biological defense mechanisms (Flower, 1996). Lipocalins are present in a wide range of organisms such as bacteria, plants, arthropods, and mammals (Flower, 1996; Sánchez et al., 2003). In our previous study, we identified a new lipocalin protein named as tributyltin-binding protein type 1 (TBT-bp1) and evaluated that there was a relation between this binding protein and the accumulation of TBT in the blood of Japanese flounder, *Paralichthys olivaceus* (Shimasaki et al., 2002).

Interestingly, TBT-bp1 and TBT combination is excreted from the fish body of Japanese flounder to outside via the skin mucus, suggesting that the lipocalins might have detoxification functions (Satone et al., 2008).

Homologs of TBT-bp1 are present in fish such as TBT-bp type 2 (TBT-bp2), alpha-1-acid glycoprotein-like protein (nrF-AGP), and male-specific protein (MSP) (Oba et al., 2007; Nakamura et al., 2009; Machnes et al., 2008). In addition, chemically induced changes in the expression of TBT-bps and their homologs were reported: Nassef et al. (2011) showed a change of TBT-bps concentrations in blood of Japanese flounder exposed to TBT-d27. TBT-bp1 homolog gene was down-regulated by exposure to bisphenol A, an endocrine-disrupting alkylphenol, in the self-fertilizing mangrove killifish, *Kryptolebias marmoratus* (Lee et al., 2007) and up-regulated by 7,12-dimethylbenz[a]anthracene, a polycyclic aromatic hydrocarbon that exhibit immunotoxicity to animals, in European eel, *Anguilla anguilla*, (Nogueira et al., 2009). These results indicated that TBT-bps and their homologs might respond to the exposure of chemicals. These homologs seem to play roles in accumulation and elimination of chemicals including TBT. However, original function of TBT-bp1 is still ambiguous.

TBT is well known as a high toxic chemical for aquatic organisms. It induces abnormal development in embryos, and deformity, in larvae, in the form of tail bent at the tip, curled, and/or shortened of Japanese medaka, *Oryzias latipes* (Hano et al., 2007; Bentivegna and Piatkowski, 1998), suggesting an inhibition of calcification. Furthermore, Suzuki et al. (2006) reported that TBT markedly inhibits fish scale alkaline phosphatase, which was a valid marker for osteoblastic activity (de Vrieze et al., 2010).

* Corresponding author. Tel.: +81 92 642 2905; fax: +81 92 642 2905.
E-mail address: yoshima@agr.kyushu-u.ac.jp (Y. Oshima).

In this study, we obtained a recombinant TBT-bp1 (rTBT-bp1) using a baculovirus expression system and silkworm larvae and we performed *in vitro* assay to elucidate rTBT-bp1 to restore the osteoblastic activity in fish scale inhibited by TBT.

2. Materials and methods

2.1. Cells and silkworm strain

The cell line Bme21 (e21–12: embryo derived) and the d17 silkworm strain (Kawakami et al., 2008) used in this study were provided by the Institute of Genetic Resources, Graduate School of Agriculture, Kyushu University, Japan. The cell line was maintained in IPL-41 medium (Invitrogen, CA, USA) with 10% fetal bovine serum. The cells were grown at 27 °C and split at an approximate ratio of 1:2 every 4–5 days. Before cell transfection, the medium was replaced by Sf-900 SFMII serum-free culture medium (Invitrogen).

Larvae of d17 silkworm strain were reared on mulberry leaves in a silkworm-rearing room under controlled environmental conditions at 25–27 °C.

2.2. Construction of mediator for expression vector

To generate pFBDEST-His6 used for gene transferring by means of Gateway reaction, the *att*R1-ccdB-*att*R2 cassette flanked by *Hind*III blunt-ended and *Xba*I sites was cleaved from pXINsect-DEST38 (Invitrogen) (Lee et al., 2007), and inserted into the *Sph*I blunt-ended/*Xba*I site of pMIB/V5-His B (Invitrogen). pMIB/V5-His B contains the V5 epitope and a polyhistidine (6× His) region. The resulting plasmid was designated as a pDEST38-His6. To amplify the DEST cassette and polyhistidine region of pDEST38-His6, polymerase chain reaction (PCR) was performed with two primers: DEST38-F and His6 + DEST38-R (Table 1). The 50-μl PCR reaction contained 5 μl of 10× KOD buffer, 5 μl of deoxyribonucleotide triphosphate(2 mM each), 1.5 μl of each primer (10 μM), 1 μl of MgSO$_4$ (25 mM), 1 μl of pMIB-DEST38 plasmid solution diluted fifty times as a template, and 1 μl of KOD-Plus DNA polymerase (1.0 U/μl; Toyobo, Osaka, Japan). The amplification profile was as follows: 94 °C for 2 min, and then 25 cycles at 94 °C for 15 s, 57 °C for 30 s, and 68 °C for 2 min, and then 72 °C for 10 min. The PCR product digested with *Hind*III was cloned into the *Bam*HI blunt-ended/*Hind*III site of the donor plasmid pFastBacI (Invitrogen), which contains the polyhedrin promoter and the mini-Tn7 element for transposon reaction. The resulting pFBDEST-His6 plasmid was introduced into *E. coli* DB3.1 for amplification and extracted using by means of a PlasmidSVmini kit (Geneall, Seoul, Korea).

2.3. Construction of the Gateway entry clone

To obtain the cDNA sequence of TBT-bp1, total RNA extracted from Japanese flounder (*Paralichthys olivaceus*) (Satone et al., 2008) was used as a template for reverse transcription reaction with the SuperScript III First-strand Synthesis System for RT-PCR (Invitrogen). To amplify the cDNA, PCR was performed with two primers, TBT-bp1-F and TBT-bp1-R (Table 1). The PCR reaction was carried out as described above with appropriate primers. The amplification

profile consisted of a heat denaturation as follows: 94 °C for 2 min, and then 30 cycles at 94 °C for 15 s, 60 °C for 30 s, and 68 °C for 1 min, and then 72 °C for 10 min. The PCR product digested with *Xho*I was cloned into the *Nco*I blunt-ended/*Xho*Isite of pENTR11 (Invitrogen) containing the *att*L1-*att*L2 sequence for Gateway technology. The inserted sequence was confirmed by DNA sequencing (CEQ8800 genetic analysis system, Beckman Coulter, CA, USA). To enable the protein product to fuse to the 6-histidine tag at the C-terminus of the open reading frame of the destination vector, the stop codon in the inserted sequence was removed via site-directed mutagenesis using appropriate oligodeoxynucleotides.

2.4. Generation of recombinant baculovirus

The TBT-bp1 cDNA cloned into pENTR11 was transposed to the destination vector pFBDEST-His6 by means of Gateway LR clonase reaction according to the manufacture's instructions (Invitrogen). The obtained pFBTBT-bp1-His6 transfer vector was transformed into *E. coli* BmDH10Bac (Motohashi et al., 2005). Through *in vivo* transposition mediated by Tn7 transposase, the TBT-bp1 cDNA tagged with 6× His was transferred into the mini-attTn7 target site of the baculovirus shuttle vector (bacmid). After the analysis of the inserted TBT-bp1 gene by means of PCR with M13 forward and M13 reverse primers, isolated recombinant bacmid DNA was purified with a FlexiPrep kit (GE Healthcare Bioscience, Piscataway, USA). The recombinant bacmid DNA (BmNPV/TBT-bp1-His6) was transfected into *Bombyx mori* Bme21 cells (9 × 10^5 cells per well) by the lipofection method with the CellFECTIN reagent (Invitrogen) for 6 h. The cells were incubated for 5 days, after which the recombinant initial passage (P1) viral solution was collected and stored at 4 °C. In addition, Bme21 cells were infected with P1 viral stock to generate a high-titer (P2) stock. A P3 stock was generated from the P2 stock in a similar manner. Virus stocks were maintained and titrated according to the standard protocols (O'Reilly et al., 1992).

2.5. Expression and purification of fusion protein

Larvae on day 3 of the fifth instar were carefully injected into a hemocoel with the recombinant BmNPV/TBT-bp1-His6 baculovirus by means of a microliter syringe with a 30-gauge needle (Hamilton Co., NV, USA). Four days after infection, larval legs were cut and hemolymph was collected from each larva. The collected hemolymph was diluted with binding solution (50 mM sodium phosphate, 0.3 M NaCl, 20 mM imidazole, 10% glycerol, 10 mM 2-mercaptoethanol, 1 mM phenylmethylsulfonyl fluoride, Complete EDTA-free protease inhibitor cocktail [1 tablet/100 ml], 20 mM 1-phenyl-2-thiourea; pH 7.0) and centrifuged at 2500 × g for 5 min. The supernatant was filtrated through a 0.45-μm membrane filter (Millipore, MA, USA) and applied to a HisTrap HP column (GE Healthcare Bioscience). The recombinant protein was eluted with a linear solvent gradient (50, 150 and 450 mM imidazole). Fractions containing TBT-bp1 were pooled, concentrated by ultrafiltration using Amicon Ultra-15 filter devices (10,000 NMWL membrane; Millipore) and separated by gel filtration chromatography on a TSK gel G2000SWxl column (7.8 cm × 30 cm; TOSOH, Tokyo, Japan) equilibrated with 50 mM sodium phosphate buffer (pH 7.0) containing 300 mM NaCl. The sample was eluted with the same buffer at a flow rate of 0.6 ml/min and fractionated at 1-min intervals. Fractions were analyzed by sodium dodecyl sulfate–polyacrylamide gel electrophoresis (SDS–PAGE) with the method described in our previous study (Satone et al., 2008). After electrophoresis, the running gel was immersed in fixing solution (50% ethanol, 10% acetic acid for 30 min and then stained with Coomassie Brilliant Blue R-250 (Quick-CBB; Wako, Japan). N-terminal amino acid sequencing of each band was performed by Edman degradation (Edman, 1950)

Table 1
List of primers used for this study.

Primer name	Primer sequence (5′–3′)
DEST38-F	ATCCTCGATCACAAGTTTGTACAAAAAAGC
His6 + DEST38-R	AAACTAAGCTTTAGTCAGATAAACTCAATG
TBT-bp1-F	AAATCTGTGGCTCACCTCTCACTTCCTGGTT
TBT-bp1-R	CTGACGACCCTCGAGCTTCTTCTTCAGGAG